ELSEVIER

Contents lists available at ScienceDirect

Environmental Pollution

journal homepage: www.elsevier.com/locate/envpol





Enhancing anthropogenic NMVOC emission speciation for European air quality modelling

Kevin Oliveira a^{lo}, Marc Guevara a^{lo}, Jeroen Kuenen b^{lo}, Oriol Jorba a^{lo}, Carlos Pérez García-Pando a,c^{lo}, Hugo Denier van der Gon b^{lo}

- ^a Barcelona Supercomputing Center, Plaça Eusebi Güell 1-3, Barcelona, 08034, Spain
- ^b Department of Climate, Air and Sustainability, TNO, Princetonlaan 6, Utrecht, 3584 CB, The Netherlands
- c ICREA, Catalan Institution for Research and Advanced Studies, Barcelona, 08010, Spain

ARTICLE INFO

Keywords: Non-methane volatile organic compounds Anthropogenic emissions Air pollution Model evaluation Ozone modelling

ABSTRACT

Non-Methane Volatile Organic Compounds (NMVOCs) impact health and air quality, contributing to ozone and secondary organic aerosols (SOA). With stricter pollutant limits and a growing emphasis on modelling under the new European Ambient Air Quality Directive, improving NMVOC representation — particularly in terms of speciation — is essential. Current state-of-the-art European inventories rely on outdated data, potentially limiting accuracy. This study assesses for the first time the CAMS-REGv7.1 NMVOC emission inventory across Europe and evaluates the impact of replacing its default speciation with a more recent alternative using the MONARCH chemical transport model, comparing results with benzene, toluene and xylene observations for 2019. The impact of changing the speciation on modelled O₃ is also quantified.

The updated speciation shows significant changes in emissions across NMVOC species, with all species showing changes greater than ± 15 %, significantly affecting their spatial distribution and sector contributions. Air quality modelling results show notable improvements for benzene (average NMB from -46.1 % to -27.7 %), primarily driven by a better split of residential wood combustion NMVOC proposed in this work. For toluene and xylenes, major overestimations previously observed in capital cities are largely reduced by improving the characterisation of solvent activities with the new speciation profiles. However, some areas showed degraded performance likely due to the over-allocation of industrial emissions in urban areas, limiting the assessment of speciation changes and worsening the overall underestimation. Despite significant changes in the split of NMVOCs, the proposed changes show minimal impact on modelled O_3 levels, aside from localised spatial and temporal variability. The largest daily variations in MDA8 were -14 μ g/m³ in March and +8 μ g/m³ in May. The effects are smaller during summer, possibly due to an increasing role from biogenic emissions. Additional measurements of NMVOC species, along with more detailed model mechanisms, are needed to extend the evaluation.

1. Introduction

Non-methane Volatile organic compounds (NMVOCs), emitted from both natural (Sindelarova et al., 2022; Trimmel et al., 2023) and anthropogenic sources (Chen et al., 2023; Duan et al., 2023), are of increasing concern due to their significant impacts on air quality and public health. Some species, such as benzene, are known carcinogens, while others can damage the central nervous system, respiratory system, and liver (Alford and Kumar, 2021; Shuai et al., 2018; Zhou et al., 2023). Additionally, NMVOCs undergo photochemical oxidation in the atmosphere, leading to the formation of ozone (O₃) (Atkinson, 2000; Butler et al., 2011; Monks et al., 2015) and secondary organic aerosols (SOA) (Ye et al., 2024; Srivastava et al., 2022; Heald and Kroll,

2020), which significantly contribute to the particulate matter (PM) levels in the atmosphere (Chen et al., 2022; Huang et al., 2014). These substances pose further risks, with O₃ affecting human health, climate, vegetation, and crops (Xiong et al., 2024; Tai et al., 2021; Lelieveld et al., 2015; Mills et al., 2016), and PM contributing to a wide variety of adverse health problems (Juginović et al., 2021; Thangavel et al., 2022; Stackelberg et al., 2013).

With the new European Ambient Air Quality Directive 2024/2881/EU setting stricter O_3 and PM limit and target values (EC, 2024), the importance of accurately assessing NMVOC emissions to control them has increased (Petetin et al., 2023; Xiao et al., 2024; Zhang et al., 2022). However, due to the complexity of NMVOCs, their emissions remain

E-mail address: kevin.deoliveira@bsc.es (K. Oliveira).

^{*} Corresponding author.

poorly understood (Desservettaz et al., 2023; Pozzer et al., 2022). Several factors contribute to the uncertainties in NMVOC emission estimates. First, total emission estimates rely on emission factors (EF) and activity data that can vary widely and are often based on limited or outdated information (von Schneidemesser et al., 2023). Second, uncertainties arise from the spatial and temporal disaggregation of emissions (Guevara et al., 2021; Navarro-Barboza et al., 2024). Lastly, the speciation profiles, which split total NMVOCs into specific species, are crucial for evaluating individual components. Yet, these profiles often show inaccuracies due to a lack of detailed source-specific measurements needed for their update. Current literature frequently relies on non-specific and outdated speciation profiles, mainly obtained in the 1990s, which are highly sensitive to factors such as location, year, technology, and measurement methodology (Theloke and Friedrich, 2007; Huang et al., 2017; Passant, 2002). While the speciation for some sectors, such as combustion processes (e.g. wood, coal, or oil combustion), may not have changed significantly, sectors like solvents and transport have evolved considerably. For instance, Directive 2010/75/EU (EC, 2010), restricted solvent use, while continuous technological advancements in road transport efficiency across different EURO categories have led to substantial changes over time.

As part of the European (EU) Copernicus Atmosphere Monitoring Service (CAMS) (CAMS, 2024), the Netherlands Organisation for Applied Scientific Research (TNO) develops and maintains the European Regional emission inventory (CAMS-REG) (Kuenen et al., 2022), which provides gridded information for the main air pollutants to support the CAMS European regional air quality production system (Colette et al., 2024). Beyond its application under CAMS, the CAMS-REG inventory is also widely employed in many modelling applications and studies (Tokaya et al., 2024; Timmermans et al., 2022; Navarro-Barboza et al., 2024). Due to the scarcity of direct emission measurements, the assessments of emission estimates are often done indirectly by using them as input in atmospheric chemistry and transport models and comparing the modelling outputs against observations. While several works have focussed on assessing the quality of the CAMS-REG inventory for the main criteria pollutants, such as NO_x, PM, SO_x, CO, and NH3 (Jung et al., 2022; Skoulidou et al., 2024; Thunis et al., 2021), similar in-depth evaluation works for NMVOC emissions have not yet been conducted for this inventory. Nevertheless, recent evaluations have been carried out using other emission inventories (Oliveira et al., 2024; von Schneidemesser et al., 2023; Ge et al., 2024; Rowlinson et al., 2024).

This study assesses the impact of changing NMVOC emission speciation on air quality model performance by evaluating CAMS-REG NMVOC emissions using the Multiscale Online Nonhydrostatic AtmospheRe CHemistry (MONARCH; Badia et al. (2017), Klose et al. (2021), Pérez et al. (2011)) chemical transport model. As CAMS-REG relies on speciation profiles from the 1990s, we examine the impact of replacing them with a more recent database compiled by Oliveira et al. (2023). Modelled concentrations are compared against European in situ measurements for 2019, focusing on benzene, toluene, and xylenes (BTX) due to their relevance to health and air quality, the availability of observations, and the limitations of the current chemical mechanism in representing other individual NMVOCs (Hanif et al., 2021; Oliveira et al., 2024). The analysis also quantifies the sensitivity of O₃ to changes in NMVOC speciation.

2. Data and methods

2.1. Emissions

For this study, we used emissions from the Copernicus Atmosphere Monitoring Service Regional Anthropogenic Air Pollutants emission inventory (CAMS-REG; Kuenen et al., 2022), which covers emissions for the UNECE-Europe for the main air pollutants. We used version 7.1 of the CAMS-REG inventory for the year 2019 which contains

data reported by countries to the European Monitoring and Evaluation Programme (EMEP) in 2023, aggregated by sector and fuel type. These reported emissions are spatially distributed at a $0.05^{\circ} \times 0.1^{\circ}$ grid resolution using specific proxies. Total NMVOC emissions are further disaggregated into 25 species or species groups, as detailed in Section 2.2. More detailed information regarding the emission inventory methodology is described in Kuenen et al. (2022).

To facilitate the analysis and discussions of the emission results provided in the present work, we categorised the EU into distinct regions:

- East: Bulgaria (BGR), Czech Republic (CZE), Hungary (HUN), Poland (POL), Romania (ROU), Slovakia (SVK), Slovenia (SVN).
- North: Denmark (DEN), Estonia (EST), Finland (FIN), Iceland (ISL), Lithuania (LTU), Norway (NOR), Sweden (SWE).
- South: Cyprus (CYP), Spain (ESP), Greece (GRC), Croatia (HRV), Italy (ITA), Malta (MLT), Portugal (PRT).
- West-Central: Austria (AUT), Belgium (BEL), Switzerland (CHE), Germany (DEU), France (FRA), United Kingdom (GBR), Ireland (IRL), Luxembourg (LUX), Netherlands (NLD).

2.2. NMVOC speciation profiles

Total NMVOC emissions in CAMS-REG are provided with a speciation profile to breakdown the NMVOC emissions to 25 Global Emission Inventory Activity (GEIA) NMVOC species (Huang et al., 2017), originally developed by the REanalysis of the TROpospheric chemical composition (RETRO) project (Schultz, 2007). In this work, we compare two sets of speciation profiles for distributing these emissions: the CAMS-REG default speciation database (hereinafter referred to as CAMS) and the speciation profiles compiled by Oliveira et al. (2023) (hereinafter referred to as OLIV23).

CAMS is based on an earlier report by Olivier et al. (1996) and subsequent work by Theloke and Friedrich (2007). For the sector–fuel combinations currently included in CAMS-REG, the default speciation relies on 30 unique profiles. The profiles are not country-dependent due to limited detailed data; however, for fuel-dependent sectors, the shares may vary across countries due to differences in fuel composition, which affects the final speciation share.

OLIV23 covers over 900 individual NMVOC species and incorporates recent studies on major sources, including Heeley-Hill et al. (2021) for domestic solvent use, Stockwell et al. (2015) for agricultural waste burning, and Marques et al. (2022) for passenger cars, among others. For less significant sources or those expected to remain stable over time due to the absence of new data, it occasionally relies on Passant (2002) and Theloke and Friedrich (2007). The speciation catalogue accounts for a total of 54 unique sector-fuel profiles. To allow for comparisons with the current CAMS default speciation, we linked each individual NMVOC species to the corresponding GEIA group based on the chemical formulas provided in Huang et al. (2017). Species that could not be linked to one of the 25 groups were assigned to the 'Other NMVOC (voc25)' category. As part of this work, we updated the original speciation profile proposed for the residential wood combustion (RWC) sector in Oliveira et al. (2023) to better capture the sector's nuances. Details on this update are provided in section 1 of the Supplementary Material.

The OLIV23 NMVOC speciation file constructed for this study can be obtained from Oliveira et al. (2025). The file follows the same format as the speciation file provided by default with the CAMS-REG emission inventory, with profiles categorised by country, GNFR sector, year and the GEIA 25 species.

2.3. Air quality modelling system

The air quality modelling system used in this study integrates two models: the High-Elective Resolution Modelling Emission System version 3 (HERMESv3; Guevara et al., 2019), which process the CAMS-REGv7.1 anthropogenic emissions described in Section 2.1, and the chemical transport model Multiscale Online Nonhydrostatic AtmospheRe CHemistry (MONARCH; Badia et al., 2017; Klose et al., 2021), which simulates the production, transport and removal of air pollutants.

HERMESv3 was used to regrid CAMS-REGv7.1 emissions horizontally from their original resolution $(0.1^{\circ} \times 0.05^{\circ})$ to our user-defined grid $(0.1^{\circ} \times 0.1^{\circ})$ and vertically across 24 layers, making use of the sector-dependent vertical profiles provided by CAMS-REG (Bieser et al., 2011). For the temporal disaggregation, the sector-, country- and pollutant-dependent CAMS-REG-TEMPOv3.2 profiles (Guevara et al., 2021) were used to convert the original CAMS-REG annual emissions to an hourly resolution. To prepare the emission input files required by MONARCH, HERMESv3 splits the air pollutants from CAMS-REG into the species required by the Carbon Bond 5 (CB05; Yarwood et al., 2005) chemical mechanism. For NMVOCs, the split was performed using the speciation profiles described in Section 2.2. The mapping between the GEIA and CB05 NMVOC species was performed following Guevara et al. (2019). Biogenic emissions are estimated using MEGANv2.04 (Guenther et al., 2006, 2012), which is fully integrated within MONARCH.

MONARCH is an online system for simulating atmospheric chemistry, integrating a gas-phase module with a hybrid sectional-bulk aerosol module to model tropospheric chemistry. It operates with the Nonhydrostatic Multiscale Model on the B-grid (NMMB) meteorological core (Janjic and Gall, 2012). Photolysis rates are calculated using the Fast-J scheme, accounting for clouds, aerosols, and O_3 (Wild et al., 2000). Gas dry deposition is modelled using a resistance-based approach (Wesely, 1989), while scavenging and wet deposition follow the methods of Byun and Ching (1999), Foley et al. (2010).

The gas-phase chemistry in MONARCH solves the CB05 chemical mechanism extended with chlorine chemistry (Sarwar et al., 2012). The core CB05 mechanism considers 51 chemical species, including 15 VOCs, and solves 156 reactions. It is well-suited for a range of tropospheric conditions, from urban to remote environments. Further details on MONARCH are available in the referenced sources, while the information on BTX reactions is provided in Oliveira et al. (2024).

In this study, MONARCH was configured with a rotated latitude-longitude projection at a spatial resolution of 0.1° by 0.1°, centred over the European CAMS domain, which spans 30° N to 72° N and 30° W to 60° E, covering all European countries, Turkey, part of North Africa, the European part of Russia, and part of the Middle East. The model used 24 vertical layers, extending up to 50 hPa, with HERMESv3 configured to match this vertical resolution. Meteorological boundary conditions were sourced from European Centre for Medium-Range Weather Forecasts (ECMWF) Reanalysis v5 (ERA5; Hersbach et al., 2023) for 2019, while boundary condition chemistry relied on CAMS global atmospheric composition reanalyses and ECMWF's Integrated Forecasting System (IFS; Flemming et al., 2015).

2.4. Observations

To evaluate the performance of MONARCH in modelling NMVOC concentrations, we used the data compiled for the year 2019 from the Globally Harmonised Observations in Space and Time (GHOST; Bowdalo et al., 2024). For measured BTX concentrations, the primary data source was the EEA Air Quality e-Reporting (EEA, 2023). This dataset was complemented with additional data from existing national and subnational networks: for Spain, we used data provided by MITECO (MITERD, 2020), which increased the number of stations for benzene from 73 to 121, for toluene from 40 to 54, and for xylenes

from 20 to 62; for the Netherlands, we included data reported by RIVM (RIVM, 2024), which increased the number of stations for benzene from 5 to 15, for toluene from 5 to 15, and for xylenes from 0 to 9; and for the Paris area, we incorporated data from Airparif (Airparif, 2024), which increased the number of stations in France for benzene from 13 to 31, for toluene from 9 to 27, and for xylenes from 0 to 22. After incorporating these sources, the compiled dataset consisted of 672 stations monitoring benzene, 256 stations for toluene, and 238 stations for xylenes.

To improve the dataset's quality, we implemented temporal coverage criteria, retaining only those stations with at least 75% data availability. Stations with approximately less than nine months of data were excluded from the analysis to minimise the potential impact of stations with insufficient measurements. As a result of this filtering, we excluded 154 stations for benzene, 55 stations for toluene, and 46 stations for xylenes.

The compiled dataset includes measurements from various techniques, calibrations, and instruments, which introduces uncertainties that should be carefully considered when drawing conclusions (Diez et al., 2022). For example, the analysis of benzene measurement values reported in two stations in Latvia revealed significant discrepancies, with annual averages approximately seven times higher than those reported elsewhere in Europe. Further examination of these locations found no identifiable emission sources to explain the elevated values. Furthermore, we identified that these stations employed a unique measurement technique compared to the rest of the stations, i.e. differential optical absorption spectroscopy (DOAS) instead of the gas chromatography (GC)-based methods. The DOAS method can be affected by overlaps with other compounds, while GC separates compounds before detection. This difference may explain the observed discrepancies with the rest of Europe. To avoid potential misinterpretation of the data, we decided to exclude these two stations from our analysis.

Fig. 1 shows the locations of the stations monitoring BTX, along with the measured annual average concentrations. The final dataset includes 496 stations for benzene (343 urban, 109 suburban, and 44 rural), 198 stations for toluene (120 urban, 50 suburban, and 28 rural), and 170 stations for xylenes (97 urban, 46 suburban, and 27 rural). In terms of spatial coverage, Italy and Belgium are particularly notable for their extensive representation.

A brief overview of the annual averages and regional distribution of benzene, toluene, and xylenes measurements across Europe is presented in section 3 of the Supplementary Material.

3. Results

3.1. NMVOC speciated emissions comparison

In this section, we compare the speciated NMVOC emissions from CAMS-REGv7.1 after applying the two speciation profile databases: CAMS and OLIV23. It is important to note that, since only the NMVOC speciation has been modified, the total NMVOC emission sums remain unchanged. A overview of the total NMVOC emissions by region and sector is presented in section 2 of the Supplementary Material.

Table 1 presents the total emissions at the EU level per NMVOC GEIA species, along with the absolute and relative differences between the two speciations. This section focuses on discussing changes observed in BTX emissions, since these are the species considered in the air quality modelling evaluation (see Section 3.2). The remaining NMVOCs that contribute significantly to total emissions or have experienced notable changes (e.g., acids (voc24), isoprenes (voc10), monoterpenes (voc11), propane (voc03), higher alkanes (voc06), ethyne (voc09)) are discussed in section 4 of the Supplementary Material. The resulting emission changes are contextualised by comparisons with other studies (Panopoulou et al., 2020; Peng et al., 2022; Borbon et al., 2023; Dalsøren et al., 2018; Ge et al., 2024; Rowlinson et al., 2024),

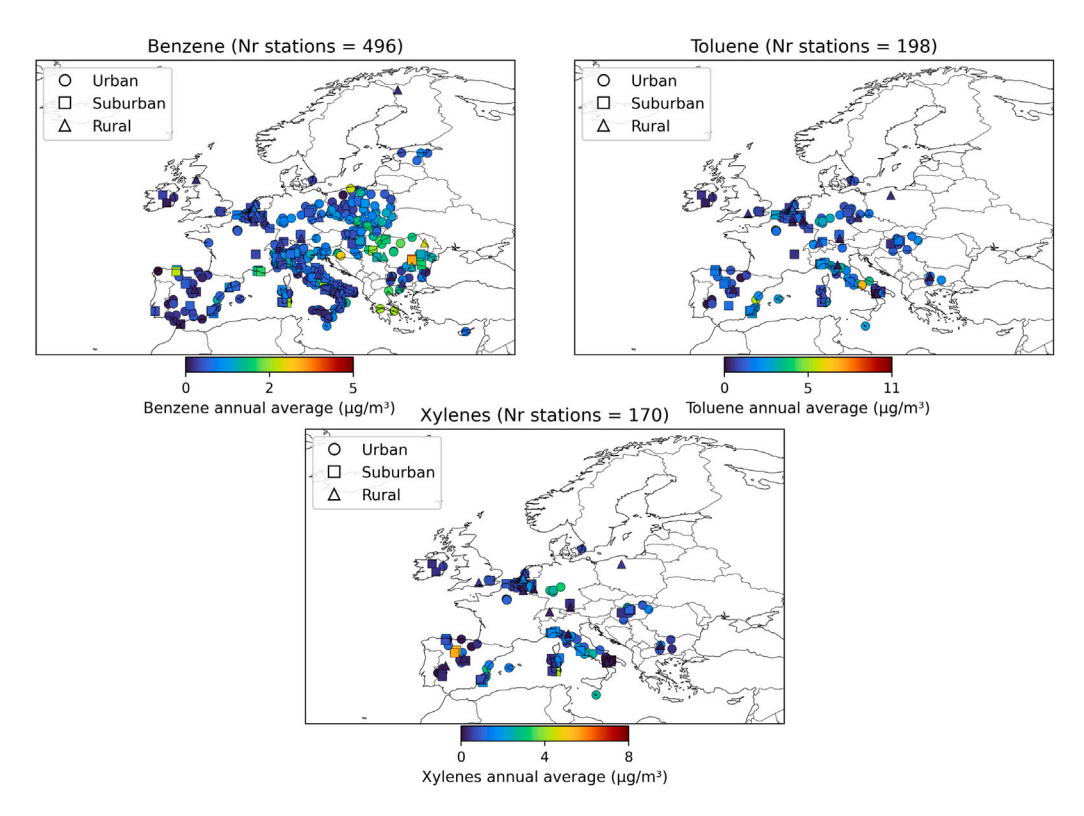


Fig. 1. Location of air quality monitoring stations measuring BTX across Europe in 2019. The area classification of each station is represented by different markers (urban, suburban, and rural), while the colour of the markers indicates the annual average concentration in $\mu g/m^3$. Only stations with more than 75% of valid data are included in the map.

Table 1

Comparison of the CAMS-REG total EU emissions for 2019 per GEIA species using CAMS and OLIV23 speciation

GEIA ID	GEIA Group	EU emissions (kt)		Differences	
		CAMS	OLIV23	(kt)	(%)
voc01	Alkanols (alcohols)	1464	1739	274	19
voc02	Ethane	186	227	41	22
voc03	Propane	129	294	165	127
voc04	Butanes	259	423	164	63
voc05	Pentanes	302	257	-45	-15
voc06	Hexanes and higher alkanes	1121	726	-395	-35
voc07	Ethene (ethylene)	298	343	45	15
voc08	Propene	89	107	18	20
voc09	Ethyne (acetylene)	80	157	77	97
voc10	Isoprenes	0	10	10	_
voc11	Monoterpenes	1	83	82	1222
voc12	Other alk(adi)enes/alkynes (olefines)	145	181	35	24
voc13	Benzene	123	188	65	53%
voc14	Methylbenzene (toluene)	336	145	-190	-57
voc15	Dimethylbenzenes (xylenes)	294	193	-100	-34
voc16	Trimethylbenzenes	22	4	-18	-83
voc17	Other aromatics	145	349	204	141
voc18	Esters	408	289	-119	-29
voc19	Ethers (alkoxy alkanes)	346	12	-334	-97
voc20	Chlorinated hydrocarbons	232	125	-107	-46
voc21	Methanal (formaldehyde)	62	86	24	39
voc22	Other alkanals (aldehydes)	196	432	236	121
voc23	Alkanones (ketones)	389	319	-71	-18
voc24	Acids (alkanoic)	450	16	-435	-97
voc25	Other NMVOC	230	605	375	163

which, despite using different models or satellite-derived data, serve as valuable references.

To complement the analysis, Fig. 2 illustrates the resulting gridded maps $(0.1^{\circ} \ x \ 0.1^{\circ})$ of annual BTX emissions, considering both CAMS and OLIV23 speciations, as well as the relative differences between them. Finally, Fig. 3 shows the absolute and relative contribution of each GNFR sector to total BTX emissions per country obtained

with each speciation. In the Supplementary Material, sections 6 and 7 provide the sectoral contributions and spatial emission maps for the remaining NMVOC GEIA species.

For benzene, other stationary combustion (GNFR C) is the dominant sector, contributing 58% in CAMS and 64% in OLIV23. Replacing CAMS with OLIV23 results in a 53% increase of total emissions at the EU level, the rise being considerably homogeneous across countries

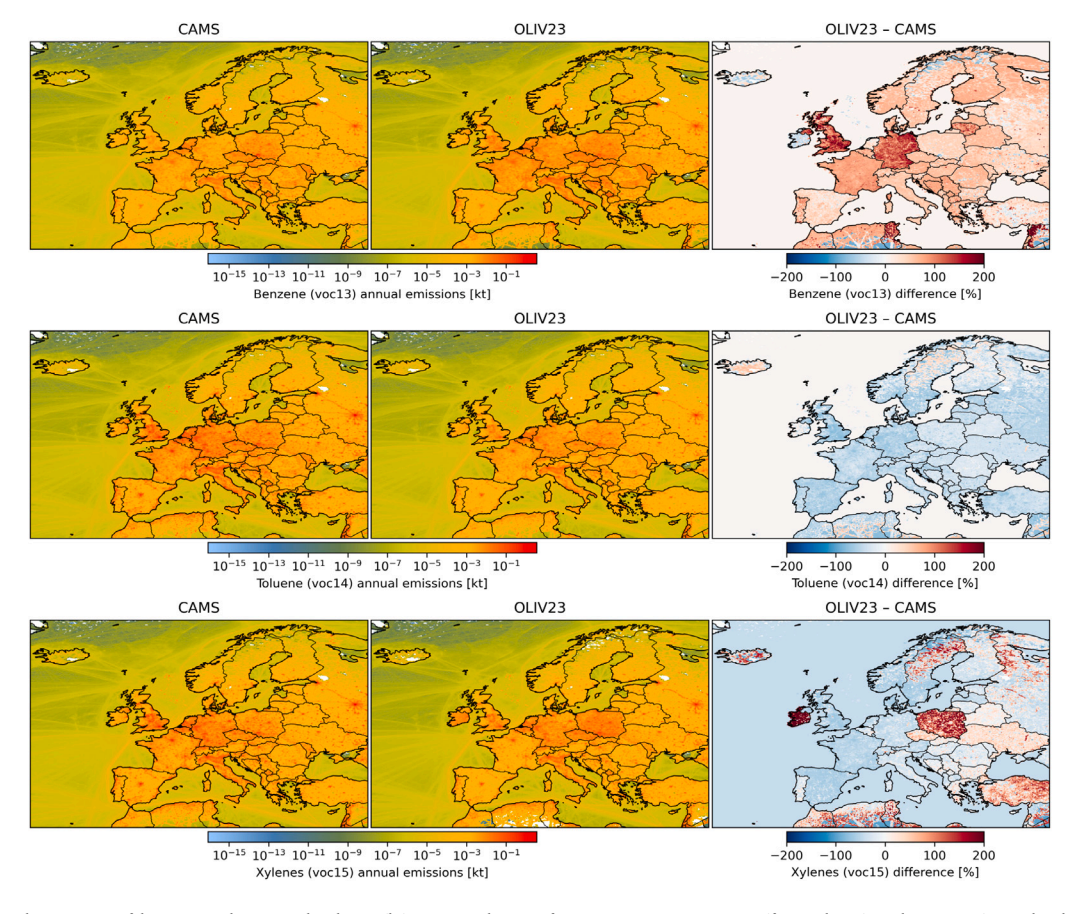


Fig. 2. Gridded annual emissions of benzene, toluene, and xylenes (kt) at a resolution of 0.1° x 0.1°, using CAMS (first column) and OLIV23 (second column), along with the relative differences between them (third column).

(Fig. 2). Notable increases are seen in Germany, the UK, and France, where emissions can rise by up to 180%, while in Ireland, decreases can reach 50 %. The increase is mainly attributed to a higher share of benzene in RWC emissions, with OLIV23 accounting for nearly twice the share (12.1%) compared to CAMS (6.8%) (Fig. 3). This aligns with literature, which identifies benzene as a key aromatic species in this source, with contributions reaching up to 34% (Chen et al., 2017; Hartikainen et al., 2018). The rise in benzene emissions in Germany, the UK, and France are mainly due to a significant increase in emissions from the Waste sector (GNFR J), particularly solid waste treatment, from 0.6 kt, 0.3 kt and 0.5 kt in CAMS to 5.9 kt, 2.4 kt and 3.7 kt with OLIV23. In CAMS, this sector is characterised by a solvent use profile with no benzene share, while OLIV23 assigns a 2.5% benzene share, sourcing from several studies related to waste management. The notable decreases in Ireland results from coal burning in other stationary combustion activities (GNFR C), with emissions dropping from 0.54 kt to 0.25 kt, as the benzene share reduces from 5% in CAMS to below 1% in OLIV23. It is also worth noting the spatially heterogeneous changes observed in Poland when moving from CAMS to OLIV23 profiles (Fig. 2). A general increase in emissions (ranging from 5 to 50%) is observed across the country, except in some localised areas, particularly in the South, where emissions decrease by around 90%. These reductions are primarily driven by a decrease in benzene fugitive emissions from coal mining activities (sector GNFR D) when moving from CAMS to OLIV23 speciation. Further analysis of these changes and associated impacts on modelled benzene concentrations can be found in Section 3.3.1.

For toluene (voc14) and xylenes (voc15), the dominant sector is the use of solvents for both CAMS and OLIV23 speciation profiles, despite their contributions to total emissions decreasing from 70% and 80% in CAMS to 34 % and 40% in OLIV23, respectively. Replacing CAMS with OLIV23 leads to a 57% and 34% decrease in toluene and xylenes

emissions at the EU level, respectively. These reductions are primarily driven by changes in the use of solvent sector profiles, particularly in domestic solvent use, coating applications, and chemical product manufacturing. For example, for the domestic solvent use sector, OLIV23 proposes a profile based on measurements performed in 2021 in 60 UK houses by Heeley-Hill et al. (2021), while CAMS assume an industrial speciation profile. While the first study suggest a 0.5% and 0.9% share of total NMVOC associated to toluene and xylenes, respectively, the CAMS profile indicates shares of approximately one order of magnitude larger (7.5% for both toluene and xylenes).

As shown in Fig. 2, toluene emissions generally decrease by -25% to -50% across most countries, with urban areas experiencing larger reductions (-65% to -80%) due to lower emissions from domestic solvent use in OLIV23. In contrast, xylenes emissions show heterogeneous changes, with increases in countries such as Ireland, Poland, and the Czech Republic, and decreases ranging from -5% in Portugal to -55% in France. The reductions are linked to the solvent sector, where the speciation changes reduce the share of most activities. In contrast, the increases are driven by coal combustion in the residential and commercial combustion sector (see Fig. 3), with shares rising from 1% in CAMS to 48% in OLIV23.

3.2. Model performance

Fig. 4 shows the time series of modelled BTX concentrations using MONARCH and CAMS-REGv7.1 emissions with the CAMS (light red line) and OLIV23 (light blue line) speciation. Modelled results are compared to observations averaged across all stations (black line). The scatter plot represents the annual average for each station, along with its corresponding area classification (i.e., urban, suburban, and rural). Appendix A presents statistical tables for each pollutant, averaged

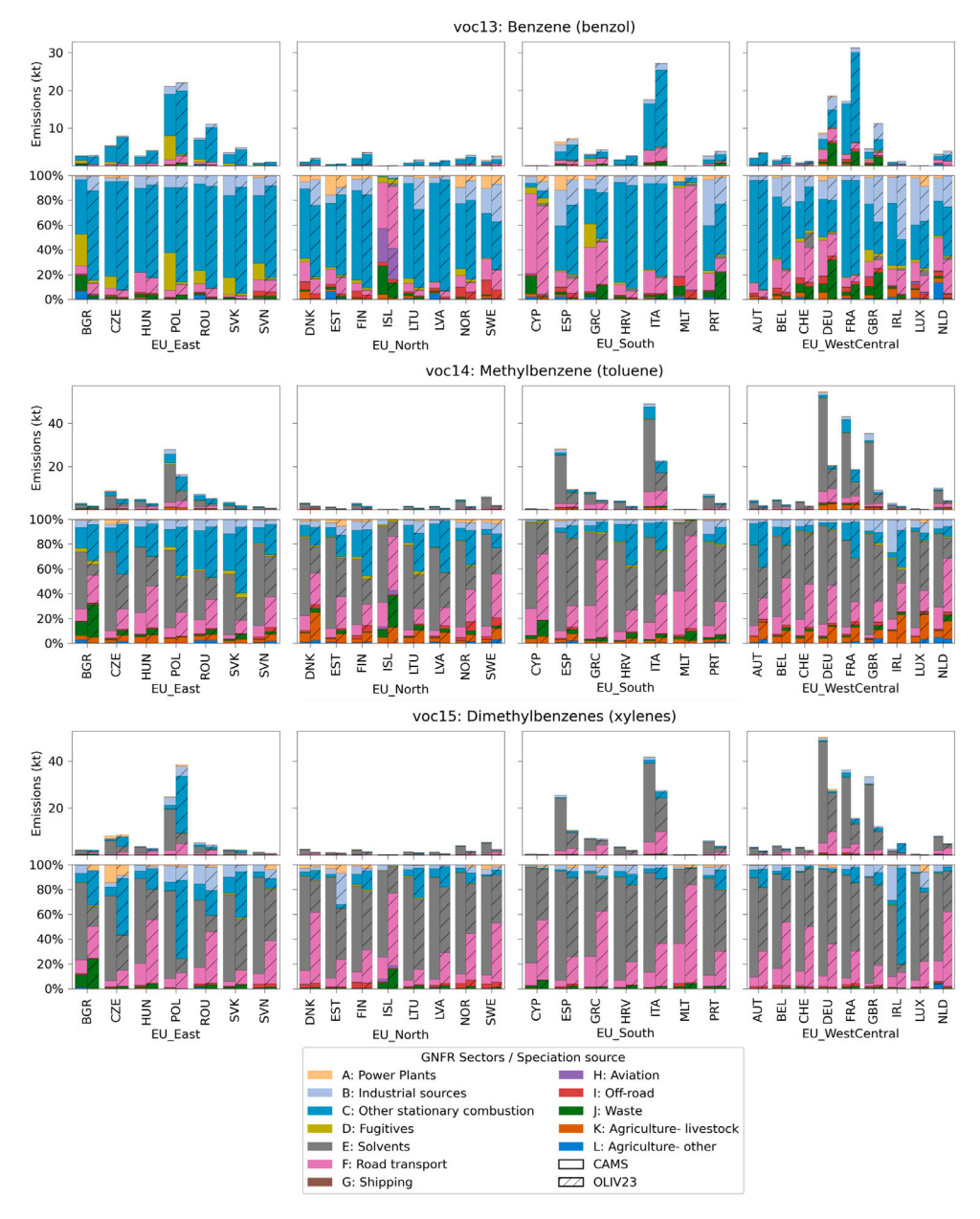


Fig. 3. Total anthropogenic BTX emissions across EU countries comparing two speciation sources, CAMS and OLIV23. The first row of each plot shows emissions in kilotons (kt) by GNFR sector within each country, while the second row presents the relative percentage contribution.

across European regions and seasons (winter (JFM), spring (AMJ), summer (JAS), and autumn (OND)). Fig. 5 displays the mean bias (MB) in $\mu g/m^3$ for each station, categorised by area classification, comparing results from both speciation datasets.

Overall, when changing the speciation profiles from CAMS to OLIV23, the benzene bias decreases, while the bias for toluene and xylenes increases due to the compensation of errors and other nuances in the emissions. This section focuses on the results using the default CAMS speciation, while the impact of replacing it with OLIV23 is discussed in greater detail in Section 3.3.1.

For benzene (Table A.2), averaged modelling results across all stations and seasons demonstrate a strong correlation (0.90) despite significant underestimations (NMB of -46.1%). This negative bias is largely driven by significant underestimation observed in the majority of stations in Italy, which is the country with the largest number of stations (n = 199). When averaged across stations per region, the North shows the worst performance with a correlation of 0.56, while the South exhibits the best with a correlation of 0.88. In terms of NMB, the

lowest value is observed in the East (NMB = -37.8%), and the highest in the North (NMB = -66.4%). This could be mainly related to the low share of emissions from residential wood combustion, which plays a significant role in the North. Seasonally, the model shows the weakest correlation during summer and the strongest during spring, except in the North, where the highest correlation occurs in winter. The poor performance during summer may indicate that emissions from other sectors are poorly characterised, whereas this is less evident in winter, when the biggest share of emissions are from RWC. However, this could also reflect the greater influence of photochemistry in summer compared to other seasons.

As illustrated in Fig. 5, several individual stations stand out, particularly in southern Poland, where one station shows the largest overestimation (MB = $6.3 \, \mu g/m^3$, NMB = 311.3%). Notably, the measured annual average at this station is $2.0 \, \mu g/m^3$, while the modelled value reaches $8.3 \, \mu g/m^3$, exceeding the annual limit value of $5 \, \mu g/m^3$ for benzene. This area is known primarily for the intense coal mining activities, and the emission hotspot shown in Fig. 2 is mainly due

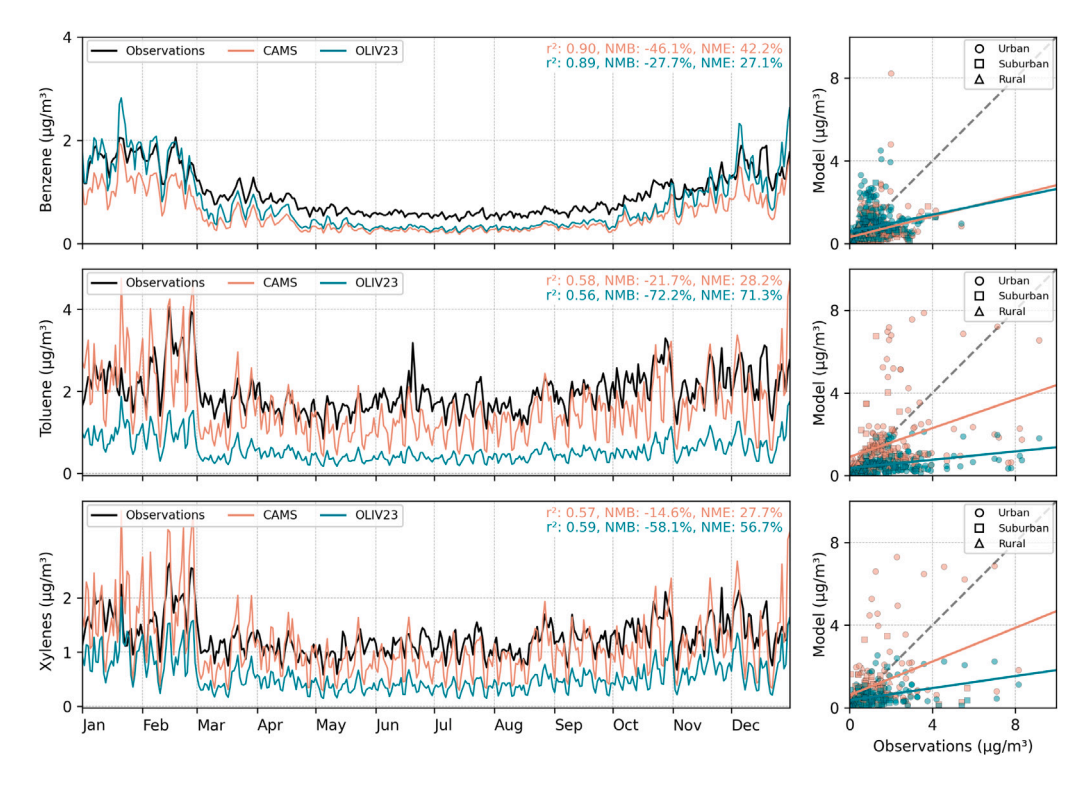


Fig. 4. On the left, averaged daily BTX concentrations $(\mu g/m^3)$ modelled and measured for all stations in 2019. On the right, scatter plots showing annual mean modelled BTX concentrations against measurements $(\mu g/m^3)$ in 2019 for each individual station, with markers indicating area classification (urban, suburban, and rural). Results are displayed for two speciation datasets: CAMS (light red) and OLIV23 (light blue), alongside observations (black).

to fugitive emissions related to this activity. Notably, changing the speciation leads to an important improvement (see Appendix B), as discussed in more detail in Section 3.3.1.

Scattered across Europe (e.g., Italy, Croatia, Hungary, Spain, and Romania), several stations exhibit underestimations not only for benzene, but also for toluene and xylenes. A detailed assessment of the station locations shows that, generally, they are situated near large industrial facilities, such as refineries and coke ovens for benzene stations, and car manufacturing plants, steel mills, paper mills, and power plants for toluene and xylenes stations. This underestimation pattern aligns with the results previously found for Spain by Oliveira et al. (2024) and can be attributed to uncertainties in the reported facilitylevel NMVOC emissions. These emissions are often based on estimation approaches (e.g., mass balance) rather than direct measurements. Additionally, the speciation profiles assigned to these facilities may not fully capture the complex nature of industrial NMVOC emissions, which typically result from combustion processes using fossil fuels, storage and distribution of products, the use and production of solvents, and other industrial processes (Farhat et al., 2024).

For both toluene (Table A.3) and xylenes (Table A.4), the model shows a similar performance, with an NMB of -21.7% and -14.6% and a correlation of 0.57 and 0.58, respectively. Regionally, the model performance shows significant variations. In both cases, the North region exhibits significant overestimations, with toluene showing an NMB of 18.4% and xylenes showing 127.2%, but it is important to note that the North only has one station, so these results are not representative of the region. The West Central region also shows overestimations for both pollutants, with toluene at 7.5% and xylenes at 29.5%, primarily driven by overestimations in major cities such as Paris and London, which are discussed in more detail later in the section. In contrast, both the East and South regions show underestimations. The South shows the largest bias for both toluene (NMB = -42.3%) and xylenes (NMB = -42.6%), predominantly influenced by stations near specific facilities in Italy and Spain. The East region shows smaller underestimations for both toluene (NMB = -14.6%) and xylenes (NMB = -9.8%), with the

weakest correlation for both pollutants (r=0.48 for toluene, r=0.47 for xylenes). The weakest correlations occur in spring for toluene (r=0.28) and in summer for xylenes (r=0.25), likely due to emission uncertainties and the model's ability to reproduce photochemistry accurately. When averaged across regions, the best correlations for both toluene (r=0.60) and xylenes (r=0.62) are found in the South. Seasonal performance is strongest in autumn for the East and South regions, while the West Central region performs best in summer.

For both species, the relatively low NMB results from a compensation effect between significant overestimations occurring in stations within major urban areas (such as Madrid, Paris, Rome, London, and Budapest, see Fig. 5) and underestimations observed elsewhere. When estimating the NMB without including stations located within the boundaries of these cities, the NMB increases significantly for both toluene (from -21.7% to -43.3%) and xylenes (-14.6% to -35.7%). Across all these cities, the solvent use sector (GNFR E) dominates, accounting for 78% to 97% of total toluene emissions and 84% to 98% of total xylenes emissions. Upon examining the solvent sector, we identified two potential causes for these high overestimations. First, the spatial proxies used in CAMS-REG to different solvent activities may introduce uncertainties, as 99% of emissions are disaggregated using a population density proxy. While this is appropriate for domestic solvent use (NFR 2D3a), which accounts for about 28% of both toluene and xylenes emissions from the solvent sector, it may not be accurate for other activities. For instance, chemical products (NFR 2D3g) and printing (NFR 2D3 h) are industrial activities, while coating applications (NFR 2D3d), other solvent use (NFR 2D3i), and other product use (NFR 2G) combine both industrial and population-based activities, with industrial accounting for the largest share. This leads to an overallocation of emissions in urban centres. Additionally, the speciation used in CAMS assigns large shares to toluene and xylenes to these activities, as previously described in Section 3.1. Thus, issues with both spatial proxies and speciation profiles contribute to the overestimations observed in major cities. While not directly evaluated in this work, these issues should also impact other species predominantly emitted by

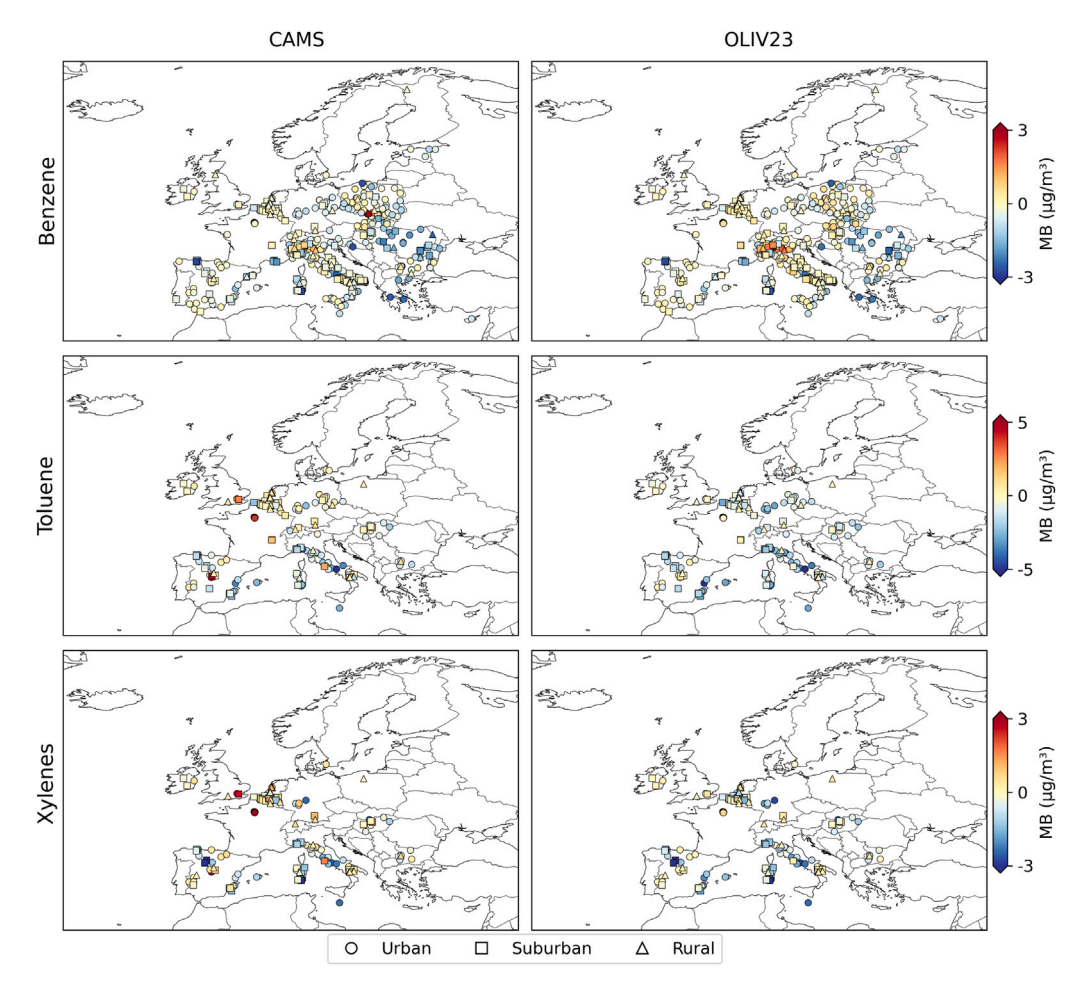


Fig. 5. Mean bias (MB) in $\mu g/m^3$ for each station for BTX, comparing the two speciation datasets: CAMS and OLIV23. Markers indicate area classification (urban, suburban, and rural).

the solvent sector, such as hexanes and higher alkanes, other aromatics, esters, ethers, chlorinated hydrocarbons, and alkanones.

3.3. NMVOC speciation sensitivity analysis

As shown in Section 3.1, changes in the speciation significantly affected the emissions of individual NMVOC species, their spatial distribution and their sectoral contributions. In some cases, while total emissions changed little, their spatial distribution still varied considerably. The following subsections evaluate the effects of these changes in reproducing observed BTX concentrations and quantify their impact on modelled $\rm O_3$.

3.3.1. BTX

For benzene, the new speciation results in significant improvements across almost all regions. Averaging over Europe (see Fig. 4), the NMB is reduced from -46.1% to -27.7%, while the temporal correlation remains almost unaltered (0.9 versus 0.89). These improvements are primarily driven by a reduction of the negative bias during wintertime, which are linked to a better characterisation of RWC emissions (see Section 3.1), which is the dominant sector for benzene during this period. The reduction of the negative bias is also evident across the other periods of the year, but to smaller degree. The South region shows the largest reduction when replacing CAMS (see Table A.2), with the NMB improving from -47.9% to -20.5% and correlation increasing from 0.56 to 0.58.

We also observe specific improvements linked to changes in benzene emissions from other sectors. For example, at a station in the South East of Poland, where emissions are dominated by fugitive sources from coal mining, using CAMS speciation, MONARCH reports the largest overestimation (6.22 $\mu g/m^3$) across stations (see Fig. 5). This overestimation is greatly reduced with OLIV23, with the NMB improving from 311.3% to -11.5% (see Fig. B.10). While reductions in benzene emissions were observed in other coal mining-dominated regions of Poland, other regions of the country showed increases linked to an increase in benzene RWC emissions (see Fig. B.9). As shown in Fig. B.11, this increase leads to a reduction in the averaged NMB across these regions, from -36.8% to -26.1%.

In Romania, Greece, and Italy, while slight improvements are observed, particularly in winter, significant biases persist even after replacing the CAMS default with OLIV23 speciation (see Fig. 5). These biases are likely associated with a combination of factors, including: (i) uncertainties in the NMVOC emissions reported for these countries, such as the high uncertainty (126%–200%) in EFs for RWC (Ministry of Environment and Energy, 2024; NEPA, 2024); (ii) country-specific characteristics not fully captured by the speciation profiles, such as differences in appliance usage (e.g., the share of fireplaces in Italy is 66%, whereas in other countries it is typically below 10%); and (iii) the ability of MONARCH to reproduce complex meteorological conditions, particularly in regions like the Po Valley (see Fig. C.12), which is known for its modelling complexities (Pernigotti et al., 2012).

For toluene and xylenes, the consistent overestimation observed with CAMS speciation in urban stations is largely reduced when moving to OLIV23 (Fig. 5), due to a more accurate emission characterisation of solvent activities, which dominate total NMVOC emissions in urban areas (Section 3.1). Fig. 6 shows the impact of this update in a selection

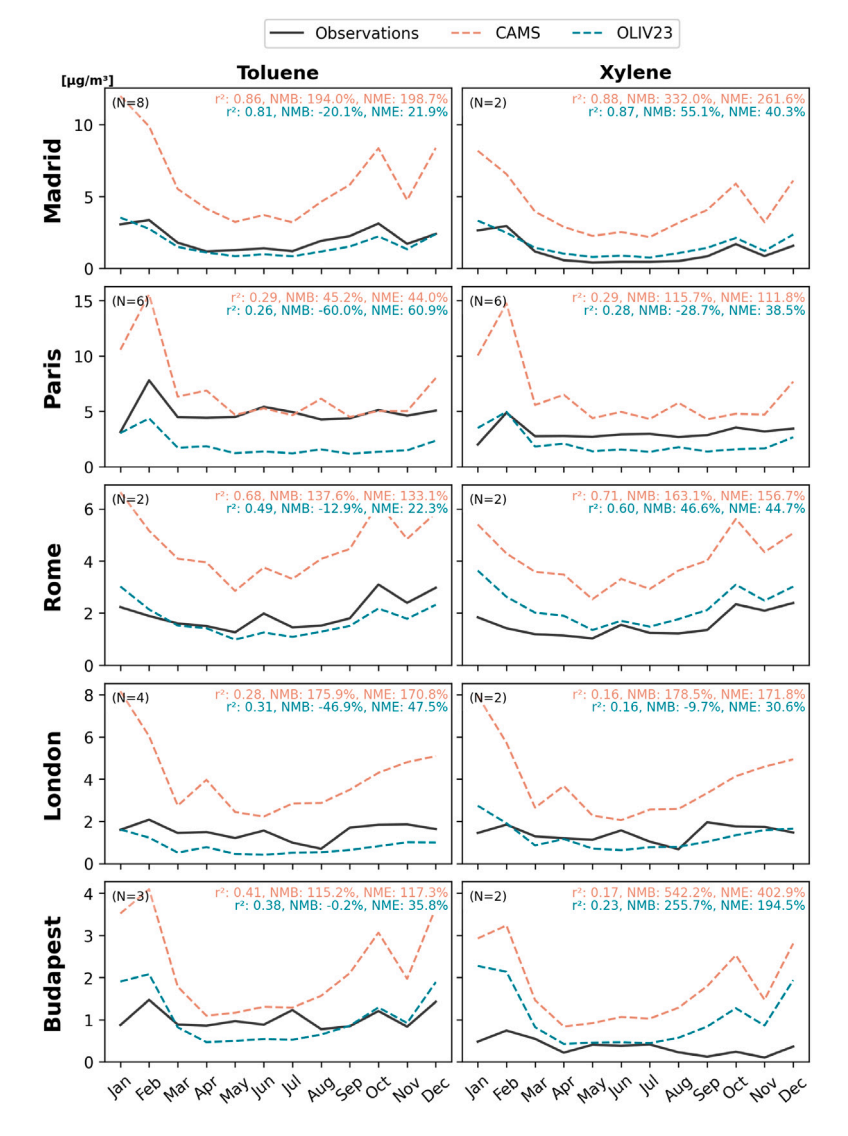


Fig. 6. Modelled and measured monthly average concentrations of toluene (left) and xylenes (right) (μg/m³) across six EU capital cities: Madrid, Paris, Rome, London, and Budapest. The plots show the observations (black), along with results from MONARCH using CAMS (light red) and OLIV23 (light blue) speciation . 'N' indicates the number of stations considered in each city.

of major European cities (Madrid, Paris, Rome, London, and Budapest). Notable reductions in NMB for both toluene and xylenes are observed when moving from CAMS to OLIV23, consistent with the reduction in urban emissions shown in Fig. 2. For toluene, the NMB decreased from 194% to -20% in Madrid, 45% to -60% in Paris, 138% to -13% in Rome, 176% to -47% in London, and 115% to 0% in Budapest. For xylenes, the NMB dropped from 332% to 55% in Madrid, 116% to -29% in Paris, 163% to 47% in Rome, 178% to -10% in London, and 542% to 256% in Budapest. However, some overestimations persist, particularly for xylenes in cities such as Madrid, Rome, and Budapest, likely due to issues with the spatial allocation of industrial solvent use emissions in the CAMS-REG inventory (see Section 3.2).

When considering all stations, the average performance of MONARCH in reproducing observed toluene and xylenes concentrations declines with OLIV23, with the NMB shifting from -21.7% to -72.2% for toluene and from -14.6% to -58.1% for xylenes (see Fig. 4). The better performance with CAMS is partly due to error compensation, where large overestimations in urban areas offset underestimations elsewhere. As shown in Fig. 7, MONARCH tends to overestimate toluene and xylenes concentrations in rural stations when using CAMS speciation. However, the NMB for xylenes improves with

OLIV23, decreasing from 46.4% to -17.4%. For toluene, the bias increases from 12.8% to -54.5%. We hypothesise that this result reflects a combination of the reduction in industrial toluene solvent emissions in OLIV23 and the over-allocation of these emissions in urban areas in CAMS-REG, as discussed in Section 3.2.

The significant negative biases for benzene, toluene, and xylenes concentration near industrial areas (see Section 3.2 and Fig. 5) persist when replacing the CAMS speciation by OLIV23. This cold bias may be partially due to uncertainties in the spatial distribution of industrial emissions in CAMS-REG. Official emissions from power plants and manufacturing industries are spatially disaggregated mainly using the E-PRTR emission database, while the remainder (i.e., differences between total emissions and E-PRTR emissions for a specific industrial sector) are distributed using area-based proxies (Kuenen et al., 2022). This approach can lead to misrepresentations, especially in those cases where a large part of the emissions are assigned to area proxies instead of specific point sources. According to CAMS-REG data, the share of emissions distributed by point source locations for specific industrial activities is as follows: 81.2% for power plants, 78.8% for refineries, 62.1% for chemical industry, 43.2% for paper mills, 29.0% for coke ovens, 20.9% for steel facilities and 0% for car coating applications.

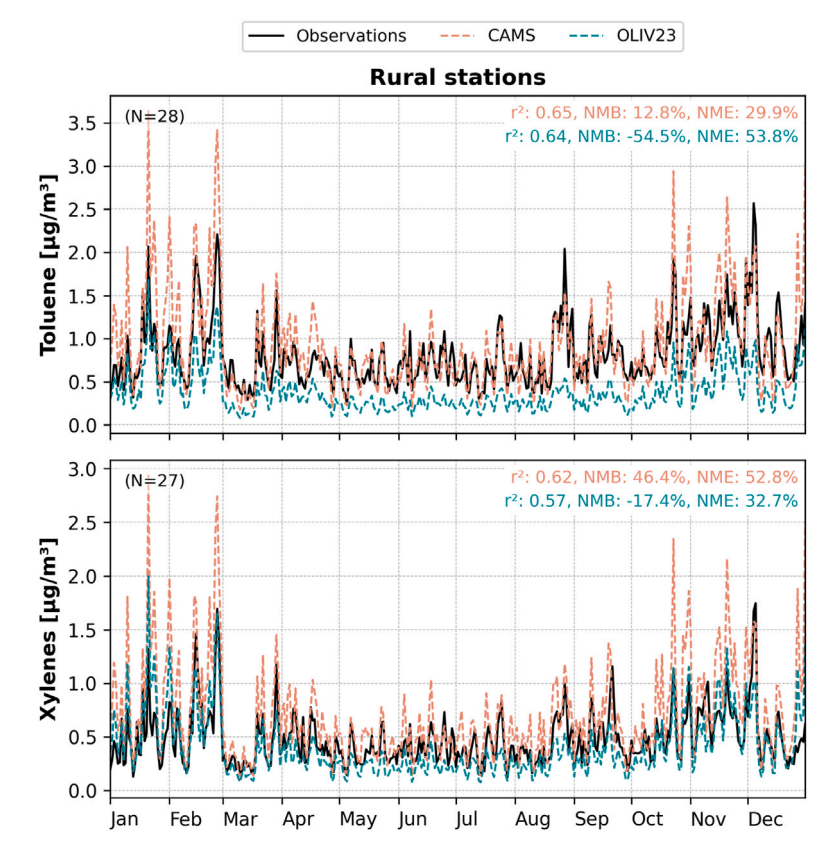


Fig. 7. Monthly average modelled and measured concentrations of toluene (top row) and xylenes (bottom row) (μg/m³) in rural stations. The plots show the observations (black), along with results from MONARCH using CAMS (light red) and OLIV23 (light blue) speciation. 'N' indicates the number of stations considered for the average.

For these activities, the remaining emissions are allocated based on industrial land uses, except for car coating applications, which use population proxies. This reliance on area-based proxies illustrates how spatial allocation of these emissions could contribute to the observed biases using both CAMS and OLIV23 speciations. In addition, while NO_x emissions reported by E-PRTR are typically based on direct measurements (at least for large point sources), NMVOC emissions are mostly derived from calculations or, in some cases, gap-filling methods due to the lack of reporting (Kuenen et al., 2022), introducing further uncertainty. Finally, it is important to note that both CAMS and OLIV23 speciations propose an NMVOC split at the GNFR sector level, not at the industrial sector level. This may introduce additional uncertainty, as substantial differences can exist between facilities (e.g., processes, fuels used) within the same GNFR sector.

3.3.2. Ozone

In this section we assess the sensitivity of O_3 modelled concentrations to the changes in the NMVOC emission speciation. We quantify the differences in the modelled maximum daily average of 8-hour O_3 concentrations (MDA8) considering CAMS and OLIV23 speciation.

The results indicate negligible average variation across the domain, with no significant changes in the intermediate percentiles (p1/p5 and p95/p99), suggesting localised effects in specific grid cells. When examining the changes in MDA8 throughout the year across the entire domain, the difference (OLIV23 - CAMS) reveals the largest reductions in minimum values, up to $-14~\mu g/m^3$ in March, and increases in maximum values, up to 8 $\mu g/m^3$ in May. These effects were less pronounced in summer (June–August: variations of -2 to 2 $\mu g/m^3$), likely because biogenic emissions dominate over anthropogenic VOCs, altering chemical regimes and reducing the sensitivity of O_3 to changes

in anthropogenic NMVOC speciation (Liaskoni et al., 2024; Miki and Itahashi, 2024). Additionally, despite significant changes in the anthropogenic emissions, the comparison of both speciations shows limited impact in terms of O₃ formation potential (OFP). We observe that OLIV23 increases the OFP by 5.5% compared to CAMS (see section 5 of the Supplementary Material), which may help explain the low overall impact.

Fig. 8 shows the spatial difference in the highest daily maximum 8-hour $\rm O_3$ concentrations (1MDA8) between CAMS and OLIV23 across the entire domain for 2019. Again, the observed impacts are quite limited. The most notable change occurs in the southern region of Poland, where a moderate decrease of around 6 $\mu g/m^3$ is linked to significant NMVOC emission changes resulting from the speciation adjustment. This change aligns with a substantial reduction in OFP in the same area, as shown in the OFP map in section 5 of the Supplementary Material. Despite this reduction, the changes do not appear to affect key metrics or exceedances at stations in the affected areas. More detailed information on the changes in MDA8 $\rm O_3$ concentrations, the fourth highest MDA8 (4MDA8), and modelled exceedances of EU and WHO $\rm O_3$ standards can be found in section 9 of the Supplementary Material.

4. Conclusions

This study evaluated the CAMS-REGv7.1 NMVOC European emission inventory spatially and temporally using the MONARCH atmospheric air quality model and a large collection of European in situ measurements for 2019. Focusing on benzene, toluene, and xylenes (BTX), we assessed the impact of replacing the CAMS default NMVOC speciation profiles with OLIV23, a more recent dataset compiled by Oliveira et al. (2023). Additionally, we analysed the impact on modelled $\rm O_3$.

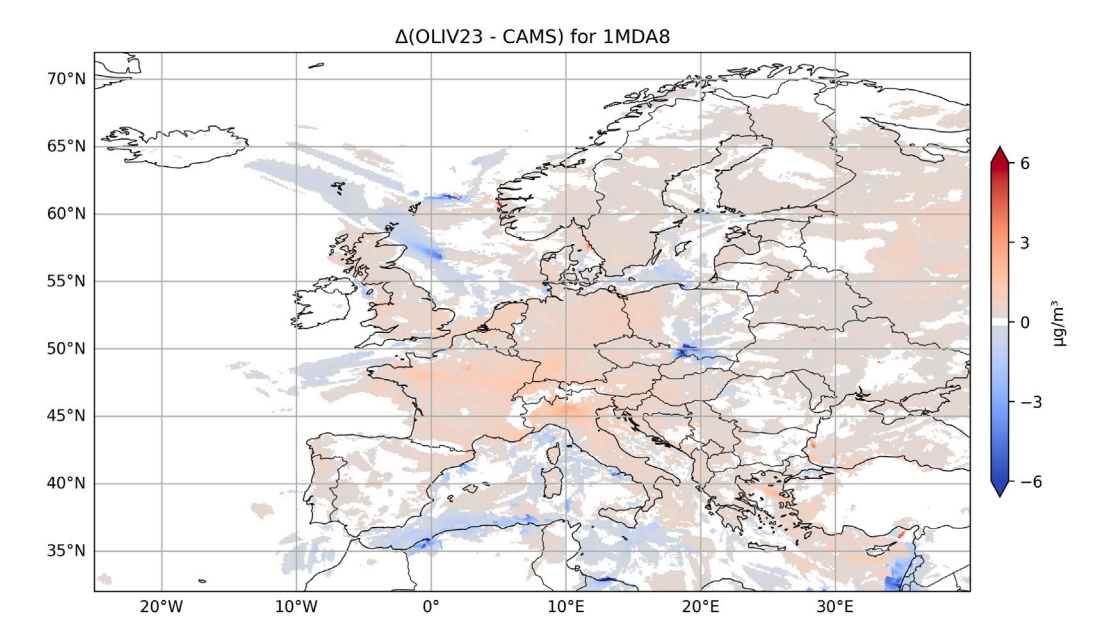


Fig. 8. Spatial difference in the highest daily maximum 8-hour O₃ (1MDA8) concentrations (μg/m³) between the baseline and alternative speciation compiled by Oliveira et al. (2023) scenarios across the entire domain for 2019.

Modifying the speciation profiles had a significant impact on individual NMVOC emissions, with all species showing changes greater than $\pm 15\%$. For several species with available literature (i.e. propane (voc03), higher alkanes (voc06), and ethyne (voc09)), the emission changes seemed to move in the right direction. However, additional measurements and further model developments are necessary to fully assess the impact of these changes on air quality modelling. Another relevant change was observed for isoprenes and monoterpenes, typically associated with biogenic sources. OLIV23 accounts for substantial anthropogenic contributions, primarily from solvent use, increasing total emissions from 1 to 93 kt. In winter, anthropogenic sources accounted for up to 36% of total monoterpene emissions in Europe, aligning with literature highlighting the growing relevance of anthropogenic sources for these species.

For benzene, the emissions are dominated by the other stationary combustion sector, specifically RWC. Changing the speciation led to a 53% increase in benzene emissions across Europe, mainly due to an increase in the share of RWC, from 6.8% in CAMS to 12.1% in OLIV23. This resulted in a significant reduction of the negative bias across the EU (average NMB improved from -46.1% to -27.7%) when using OLIV23 speciation. However, further research on RWC is needed, as some uncertainties remain, particularly concerning EFs for various RWC appliances and the speciation profile's ability to reflect country-specific characteristics. In some regions, sectoral redistribution led to emission reductions, such as in Poland, where the largest overestimations were previously observed. The reduction in coal mining emissions resulted in a notable bias reduction at that station (NMB improved from 311.3% to -11.5%).

For toluene and xylenes, replacing the speciation profiles resulted in a 57% decrease in toluene emissions and a 34% decrease in xylenes emissions, with the solvent sector remaining dominant (34% and 40%, respectively). On average, overall model performance declined, with the NMB increasing for toluene from -21.7% to -72.2% and for xylenes from -14.6% to -58.1%. However, the better performance with CAMS is partly due to error compensation, where overestimations in urban areas offset underestimations in other regions. With CAMS, significant overestimations were reported for both pollutants in major urban areas like Madrid, Paris, Rome, London, and Budapest (NMB between 45%

and 194% for toluene and between 163% and 542% for xylenes). In rural areas, the model performed better with OLIV23 for xvlenes (NMB -17.4%, compared to 46.4% with CAMS), while for toluene, the bias increased with OLIV23 (NMB changed from 12.8% to −54.5%). Additional uncertainties limit our ability to fully evaluate the nuances behind these results. The spatial allocation of CAMS-REG emissions from various solvent uses in industrial activities, such as the production of chemical products, printing, coating applications, and other solvent and product uses, is currently based on population density, leading to over-allocation in urban areas. Moreover, the model underestimates concentrations near specific industrial facilities, particularly refineries, steel mills, paper mills, coke ovens, power plants, and chemical and car manufacturing industries. This is primarily due to spatial disaggregation being carried out entirely or partially by area proxies. It is recommended that the spatial proxies used to disaggregate industrial use of solvents NMVOC emissions are revised in future versions of the CAMS-REG inventory.

In conclusion, aside from localised spatial and temporal variability, the proposed changes to NMVOC speciation have minimal impact on modelled $\rm O_3$ levels, including 1MDA8 and 4MDA8. This is consistent with previous studies Petetin et al. (2023). As noted by Garatachea et al. (2024), hemispheric contributions significantly influence air quality, potentially limiting the impact of local anthropogenic sources.

4.1. Limitations and future research

The evaluation of BTX emissions is performed indirectly through assessing the performance of an air quality model. While biases help assess emission uncertainties, model limitations in chemistry and meteorology also affect results. Another key limitation is the lack of country-specific speciation profiles, relying instead on data from other European regions. While this is practical, it introduces uncertainty, highlighting the need for further research. Additionally, attributing speciation profiles to industries may not accurately reflect the mixing of emissions from combustion and industrial processes, further contributing to uncertainty.

For other NMVOCs that have been evaluated in the existing literature, such as isoprenes, monoterpenes, propane, higher alkanes, and

ethyne, we compared emission changes with previous studies. The updated speciation aligns better with literature but presents two key challenges. First, the chemical mechanism considered in MONARCH must be updated to account for a greater number of species, as it currently only solves a limited number, some of which are lumped species. To overcome this limitation, an approach similar to the tracer method used by Ge et al. (2024) could be adopted. Second, evaluating more species requires more measurements, but the limited availability of continuous NMVOC monitoring remains a challenge. Nonetheless, several initiatives, such as the EMEP measurement campaigns (Fagerli et al., 2023) and the RI-URBANS project (https://riurbans.eu/), are emerging to address this issue.

Finally, uncertainties in the precursors, including both anthropogenic and biogenic NMVOC emissions, as well as in NO₂, chemical processes, and meteorological conditions, complicate the assessment of NMVOC impacts on O₃ levels. While the impacts on O₃ were limited, we expect a more significant influence of revised NMVOC emissions on SOA (Kelly et al., 2018), emphasising the importance of understanding its contribution to $PM_{2.5}$ concentrations.

CRediT authorship contribution statement

Kevin Oliveira: Writing – review & editing, Writing – original draft, Methodology, Data curation, Conceptualization. Marc Guevara: Writing – review & editing, Methodology, Conceptualization. Jeroen Kuenen: Writing – review & editing, Methodology. Oriol Jorba: Writing – review & editing. Carlos Pérez García-Pando: Writing – review & editing. Hugo Denier van der Gon: Writing – review & editing, Conceptualization.

Declaration of competing interest

The authors declare that they have no known competing financial interests or personal relationships that could have appeared to influence the work reported in this paper.

Acknowledgements

The present work was funded through the I+D+i project PCI2024-155065-2 funded by MICIU/AEI/10.13039/501100011033 and by the European Union; the VITALISE project (Grant No. PID2019-108086RA-IOO funded by MCIN/AEI/10.13039/501100011033); the RESPIRE project, which is part of the Recovery, Transformation and Resilience Plan (Plan de Recuperación, Transformación y Resiliencia, PRTyR) funded by the European Commission to repair the harm caused by the Covid-19 crisis. We also thank the support of the Generalitat de Catalunya Department of Research and Universities to the Atmospheric Composition Research Group (Code: 2021 SGR 01550). K. Oliveira acknowledge the support received by the grant PRE2020-092616 funded by MCIN/AEI/10.13039/501100011033 and ESF Investing in your future. The Barcelona Supercomputing Center provided computational resources at MareNostrum and technical support, while the Red Española de Supercomputación (RES) granted additional resources (AECT-2024-2-0012, AECT-2024-3-0001).

Appendix A. Model performance statistics for benzene, toluene and xylenes

See Tables A.2-A.4.

Appendix B. Poland: benzene emissions and model performance

See Figs. B.9-B.11.

Table A.2

Annual and seasonal NMB and R² for benzene obtained with MONARCH using both speciations: CAMS and OLIV23. Results are presented for Europe and each region. Seasons are defined as winter (JFM), spring (AMJ), summer (JAS), and autumn (OND).

		NMB		\mathbb{R}^2	
		CAMS	OLIV23	CAMS	OLIV23
Europe	Annual	-46.08%	-27.70%	0.90	0.89
	Winter	-32.40%	1.98%	0.57	0.53
	Spring	-52.58%	-36.25%	0.81	0.84
	Summer	-53.08%	-45.23%	0.54	0.59
	Autumn	-45.97%	-30.67%	0.78	0.75
East	Annual	-37.83%	-40.31%	0.86	0.89
	Winter	-39.19%	-21.10%	0.74	0.75
	Spring	-45.05%	-46.18%	0.78	0.79
	Summer	-30.66%	-52.14%	0.40	0.40
	Autumn	-36.42%	-41.44%	0.76	0.72
North	Annual	-66.45%	-47.10%	0.56	0.58
	Winter	-67.12%	-45.92%	0.38	0.38
	Spring	-74.07%	-59.43%	0.13	0.18
	Summer	-60.82%	-40.79%	0.11	0.13
	Autumn	-63.76%	-42.17%	0.21	0.21
South	Annual	-47.94%	-20.50%	0.88	0.88
	Winter	-26.00%	17.00%	0.56	0.55
	Spring	-54.73%	-30.55%	0.74	0.73
	Summer	-59.92%	-41.64%	0.23	0.27
	Autumn	-50.65%	-26.07%	0.70	0.68
WestCentral	Annual	-53.68%	-24.63%	0.81	0.81
	Winter	-39.79%	2.03%	0.78	0.77
	Spring	-58.28%	-33.41%	0.66	0.64
	Summer	-64.19%	-44.69%	0.58	0.56
	Autumn	-52.14%	-21.84%	0.76	0.77

Table A.3

Annual and seasonal NMB and R² for toluene obtained with MONARCH using both speciations: CAMS and OLIV23. Results are presented for Europe, as well as for each region. Seasons are defined as winter (JFM), spring (AMJ), summer (JAS), and autumn (OND).

		NMB		\mathbb{R}^2	
		CAMS	OLIV23	CAMS	OLIV23
Europe	Annual	-21.68%	-72.16%	0.58	0.56
	Winter	-3.22%	-62.83%	0.37	0.32
	Spring	-25.56%	-74.59%	0.50	0.54
	Summer	-32.78%	-77.35%	0.52	0.53
	Autumn	-24.80%	-73.68%	0.58	0.51
East	Annual	-14.57%	-57.78%	0.48	0.40
	Winter	18.97%	-32.54%	0.47	0.44
	Spring	-20.77%	-62.92%	0.28	0.27
	Summer	-33.70%	-70.99%	0.35	0.41
	Autumn	-22.13%	-64.18%	0.44	0.34
North	Annual	18.41%	-55.69%	nan	nan
	Winter	28.94%	-44.66%	nan	nan
	Spring	8.57%	-61.91%	0.46	0.48
	Summer	12.54%	-63.39%	nan	nan
	Autumn	23.85%	-52.57%	0.49	0.41
South	Annual	-42.32%	-79.18%	0.60	0.61
	Winter	-31.89%	-73.34%	0.38	0.38
	Spring	-46.62%	-81.14%	0.60	0.64
	Summer	-47.05%	-81.78%	0.29	0.31
	Autumn	-43.52%	-80.33%	0.63	0.65
WestCentral	Annual	7.53%	-63.80%	0.58	0.57
	Winter	39.84%	-50.53%	0.53	0.55
	Spring	1.86%	-67.02%	0.73	0.74
	Summer	-12.84%	-71.97%	0.73	0.78
	Autumn	1.89%	-65.42%	0.55	0.52

Appendix C. Model performance in northern Italy (Benzene, NO_2 , $PM_{2.5}$)

See Fig. C.12.

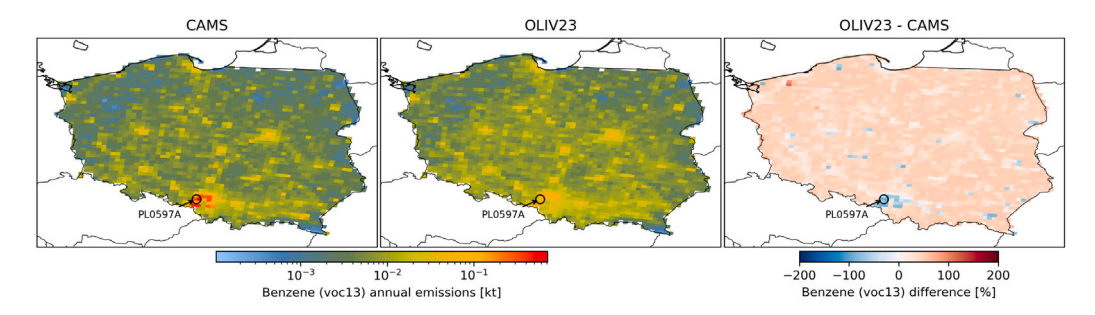


Fig. B.9. Annual gridded $(0.1^{\circ} \times 0.1^{\circ})$ benzene emissions (kt) obtained for Poland using CAMS and OLIV23 speciation. The map on the right shows the relative differences between the two results. All three maps mark the location of the EEA air quality station PL0597 A, where the largest positive bias is obtained when using CAMS speciation.

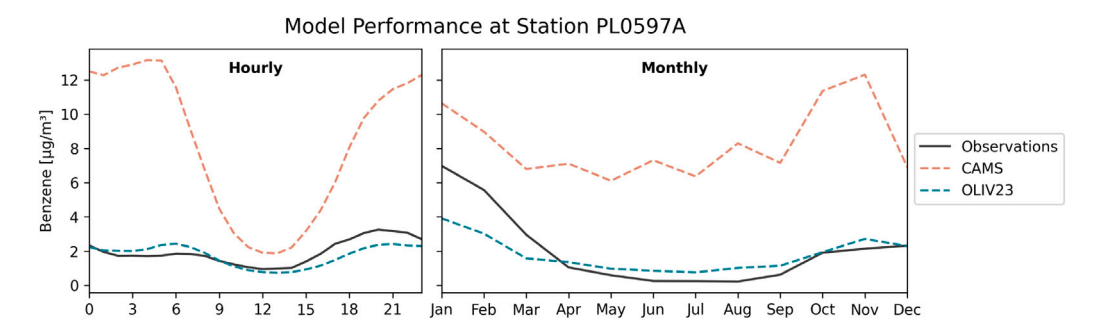


Fig. B.10. Hourly (left) and monthly (right) mean benzene concentrations ($\mu g/m^3$) measured and modelled at the EEA station PL0597 A, located in the south of Poland. Observations are shown as black lines, with MONARCH modelling results in light red for CAMS and light blue for OLIV23.

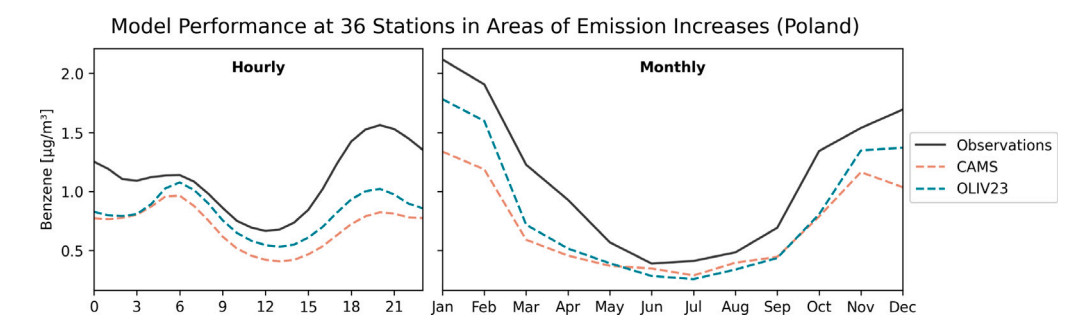


Fig. B.11. Hourly (left) and monthly (right) mean benzene concentrations (μ g/m³) measured and modelled at 36 EEA stations in Poland, where an increase in benzene emissions was observed when replacing CAMS with OLIV23. Observations are shown as black lines, with MONARCH modelling results in light red for CAMS and light blue for OLIV23 speciation.

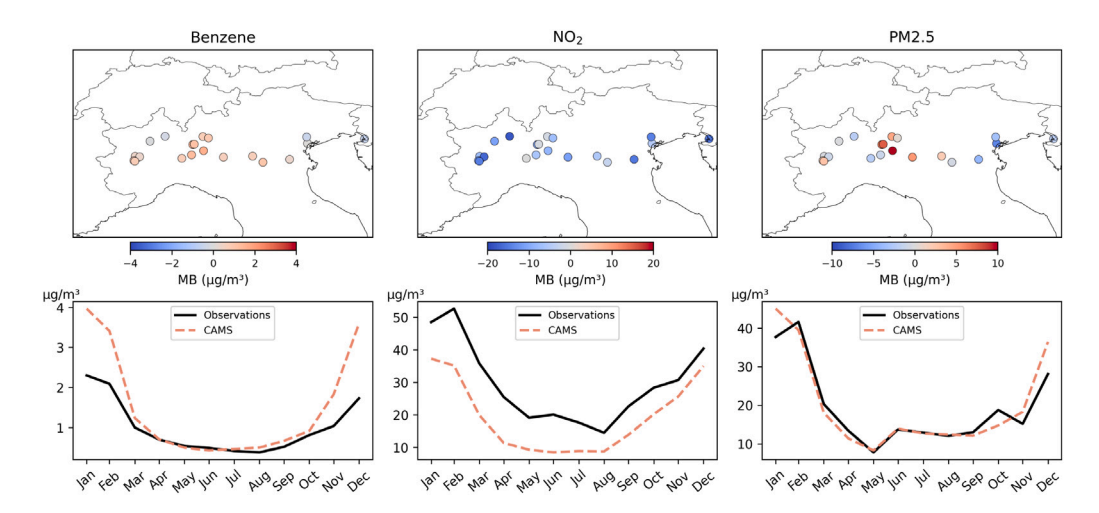


Fig. C.12. Model performance for 21 stations in Northern Italy measuring benzene, NO_2 , and $PM_{2.5}$. The top row shows the mean bias (MB), in $\mu g/m^3$, per pollutant and station. The bottom row presents the monthly average concentrations ($\mu g/m^3$) for both observations (black) and modelled data using CAMS speciation (light red).

Table A.4Annual and seasonal NMB and R² for xylenes obtained with MONARCH using both speciations: CAMS and OLIV23. Results are presented for Europe, as well as for each region. Seasons are defined as winter (JFM), spring (AMJ), summer (JAS), and autumn (OND).

		NMB		\mathbb{R}^2	
		CAMS	OLIV23	CAMS	OLIV23
Europe	Annual	-14.61%	-58.10%	0.57	0.59
	Winter	1.04%	-45.04%	0.43	0.39
	Spring	-17.07%	-61.41%	0.37	0.42
	Summer	-25.43%	-67.10%	0.59	0.61
	Autumn	-16.67%	-58.59%	0.49	0.46
East	Annual	-9.83%	-34.56%	0.47	0.35
	Winter	24.89%	17.49%	0.50	0.40
	Spring	-22.07%	-48.53%	0.46	0.37
	Summer	-35.60%	-67.33%	0.25	0.27
	Autumn	-5.73%	-38.78%	0.59	0.44
North	Annual	127.22%	7.25%	nan	nan
	Winter	161.08%	42.00%	nan	nan
	Spring	103.27%	-23.69%	nan	nan
	Summer	44.96%	-51.76%	nan	nan
	Autumn	188.18%	55.41%	nan	nan
South	Annual	-42.57%	-69.36%	0.62	0.66
	Winter	-40.11%	-64.31%	0.43	0.47
	Spring	-43.85%	-70.78%	0.44	0.44
	Summer	-45.29%	-73.04%	0.37	0.40
	Autumn	-40.98%	-69.20%	0.64	0.63
WestCentral	Annual	29.45%	-42.82%	0.53	0.53
	Winter	75.47%	-17.64%	0.50	0.50
	Spring	19.42%	-49.76%	0.63	0.64
	Summer	7.50%	-57.33%	0.64	0.66
	Autumn	16.28%	-46.04%	0.51	0.49

Appendix D. Supplementary data

Supplementary material related to this article can be found online at https://doi.org/10.1016/j.envpol.2025.126510.

Data availability

Data will be made available on request.

References

- Airparif, 2024. Airparif. URL: https://www.airparif.fr/, (Last Accessed 20 august 2024).
 Alford, K.L., Kumar, N., 2021. Pulmonary health effects of indoor volatile organic compounds—A meta-analysis. Int. J. Environ. Res. Public Heal. 18, 1578. http://dx.doi.org/10.3390/IJERPH18041578, https://www.mdpi.com/1660-4601/18/4/1578.
- Atkinson, R., 2000. Atmospheric chemistry of VOCs and NOx. Atmos. Environ. 34, 2063–2101. http://dx.doi.org/10.1016/S1352-2310(99)00460-4.
- Badia, A., Jorba, O., Voulgarakis, A., Dabdub, D., García-Pando, C.P., Hilboll, A., María, G., Janjic, Z., 2017. Description and evaluation of the multiscale online nonhydrostatic atmosphere chemistry model (NMMB-MONARCH) version 1.0: Gasphase chemistry at global scale. Geosci. Model. Dev. 10, 609–638. http://dx.doi.org/10.5194/GMD-10-609-2017.
- Bieser, J., Aulinger, A., Matthias, V., Quante, M., Gon, H.A.D.V.D., 2011. Vertical emission profiles for Europe based on plume rise calculations. Environ. Pollut. 159, 2935–2946. http://dx.doi.org/10.1016/J.ENVPOL.2011.04.030.
- Borbon, A., Dominutti, P., Panopoulou, A., Gros, V., Sauvage, S., Farhat, M., Afif, C., Elguindi, N., Fornaro, A., Granier, C., Hopkins, J.R., Liakakou, E., Nogueira, T., dos Santos, T.C., Salameh, T., Armangaud, A., Piga, D., Perrussel, O., 2023. Ubiquity of anthropogenic terpenoids in cities worldwide: Emission ratios, emission quantification and implications for urban atmospheric chemistry. J. Geophys. Res. Atmos. 128, e2022JD037566. http://dx.doi.org/10.1029/2022JD037566, URL: https://onlinelibrary.wiley.com/doi/10.1029/2022JD037566.
- Bowdalo, D., Basart, S., Guevara, M., Jorba, O., Pérez García-Pando, C., Jaimes Palomera, M., Rivera Hernandez, O., Puchalski, M., Gay, D., Klausen, J., Moreno, S., Netcheva, S., Tarasova, O., 2024. GHOST: a globally harmonised dataset of surface atmospheric composition measurements. Earth Syst. Sci. Data 16 (10), 4417–4495. http://dx.doi.org/10.5194/essd-16-4417-2024, URL: https://essd.copernicus.org/articles/16/4417/2024/.

- Butler, T.M., Lawrence, M.G., Taraborrelli, D., Lelieveld, J., 2011. Multi-day ozone production potential of volatile organic compounds calculated with a tagging approach. Atmos. Environ. 45, 4082–4090. http://dx.doi.org/10.1016/J.ATMOSENV.
- Byun, D., Ching, J., 1999. Science Algorithms of the EPA models-3 Community Multiscale Air Quality Model (CMAQ) Modeling System. Rep. EPA/600/R-99.
- CAMS, 2024. Copernicus atmosphere monitoring service. URL: https://atmosphere.copernicus.eu/, (Last Accessed 20 august 2024).
- Chen, G., Canonaco, F., Tobler, A., Aas, W., Alastuey, A., Allan, J., Atabakhsh, S., Aurela, M., Baltensperger, U., Bougiatioti, A., Brito, J.F.D., Ceburnis, D., Chazeau, B., Chebaicheb, H., Daellenbach, K.R., Ehn, M., Haddad, I.E., Eleftheriadis, K., Favez, O., Flentje, H., Font, A., Fossum, K., Freney, E., Gini, M., Green, D.C., Heikkinen, L., Herrmann, H., Kalogridis, A.C., Keernik, H., Lhotka, R., Lin, C., Lunder, C., Maasikmets, M., Manousakas, M.I., Marchand, N., Marin, C., Marmureanu, L., Mihalopoulos, N., Močnik, G., Necki, J., O'Dowd, C., Ovadnevaite, J., Peter, T., Petit, J.E., Pikridas, M., Platt, S.M., Pokorná, P., Poulain, L., Priestman, M., Riffault, V., Rinaldi, M., Różański, K., Schwarz, J., Sciare, J., la Simon, L., Skiba, A., Slowik, J.G., Sosedova, Y., Stavroulas, I., Styszko, K., Teinemaa, E., Timonen, H., Tremper, A., Vasilescu, J., Via, M., Vodička, P., Wiedensohler, A., Zografou, O., Minguillón, M.C., Prévôt, A.S., 2022. European aerosol phenomenology 8: Harmonised source apportionment of organic aerosol using 22 year-long ACSM/AMS datasets. Environ. Int. 166, 107325. http://dx.doi.org/10.1016/J.ENVINT.2022.
- Chen, J., Li, C., Ristovski, Z., Milic, A., Gu, Y., Islam, M.S., Wang, S., Hao, J., Zhang, H., He, C., Guo, H., Fu, H., Miljevic, B., Morawska, L., Thai, P., LAM, Y.F., Pereira, G., Ding, A., Huang, X., Dumka, U.C., 2017. A review of biomass burning: Emissions and impacts on air quality, health and climate in China. Sci. Total Environ. 579, 1000–1034. http://dx.doi.org/10.1016/J.SCITOTENV.2016.11.025.
- Chen, Y., Liu, C., Su, W., Hu, Q., Zhang, C., Liu, H., Yin, H., 2023. Identification of volatile organic compound emissions from anthropogenic and biogenic sources based on satellite observation of formaldehyde and glyoxal. Sci. Total Environ. 859, 159997. http://dx.doi.org/10.1016/J.SCITOTENV.2022.159997.
- Colette, A., Collin, G., Besson, F., Blot, E., Guidard, V., Meleux, F., Royer, A., Petiot, V., Miller, C., Fermond, O., Jeant, A., Adani, M., Arteta, J., Benedictow, A., Bergström, R., Bowdalo, D., Brandt, J., Briganti, G., Carvalho, A.C., Christensen, J.H., Couvidat, F., D'Elia, I., D'Isidoro, M., Denier van der Gon, H., Descombes, G., Di Tomaso, E., Douros, J., Escribano, J., Eskes, H., Fagerli, H., Fatahi, Y., Flemming, J., Friese, E., Frohn, L., Gauss, M., Geels, C., Guarnieri, G., Guevara, M., Guion, A., Guth, J., Hänninen, R., Hansen, K., Im, U., Janssen, R., Jeoffrion, M., Joly, M., Jones, L., Jorba, O., Kadantsev, E., Kahnert, M., Kaminski, J.W., Kouznetsov, R., Kranenburg, R., Kuenen, J., Lange, A.C., Langner, J., Lannuque, V., Macchia, F., Manders, A., Mircea, M., Nyiri, A., Olid, M., Pérez García-Pando, C., Palamarchuk, Y., Piersanti, A., Raux, B., Razinger, M., Robertson, L., Segers, A., Schaap, M., Siljamo, P., Simpson, D., Sofiev, M., Stangel, A., Struzewska, J., Tena, C., Timmermans, R., Tsikerdekis, T., Tsyro, S., Tyuryakov, S., Ung, A., Uppstu, A., Valdebenito, A., van Velthoven, P., Vitali, L., Ye, Z., Peuch, V.-H., Rouïl, L., 2024. Copernicus atmosphere monitoring service - regional air quality production system v1.0. EGUsphere 2024, 1-92. http://dx.doi.org/ 10.5194/egusphere-2024-3744, URL: https://egusphere.copernicus.org/preprints/ 2024/egusphere-2024-3744/.
- Dalsøren, S.B., Myhre, G., Hodnebrog, O., Myhre, C.L., Stohl, A., Pisso, I., Schwietzke, S., Höglund-Isaksson, L., Helmig, D., Reimann, S., Sauvage, S., Schmidbauer, N., Read, K.A., Carpenter, L.J., Lewis, A.C., Punjabi, S., Wallasch, M., 2018. Discrepancy between simulated and observed ethane and propane levels explained by underestimated fossil emissions. Nat. Geosci. 11:3, 178–184. http://dx.doi.org/10.1038/s41561-018-0073-0, URL: https://www.nature.com/articles/s41561-018-0073-0, 11.
- Desservettaz, M., Pikridas, M., Stavroulas, I., Bougiatioti, A., Liakakou, E., Hatzianastassiou, N., Sciare, J., Mihalopoulos, N., Bourtsoukidis, E., 2023. Emission of volatile organic compounds from residential biomass burning and their rapid chemical transformations. Sci. Total Environ. 903, http://dx.doi.org/10.1016/J.SCITOTENV. 2023.166592, 166592-166592. URL: https://typeset.io/papers/emission-of-volatile-organic-compounds-from-residential-3qtay9qh30.
- Diez, S., Lacy, S.E., Bannan, T.J., Flynn, M., Gardiner, T., Harrison, D., Marsden, N., Martin, N.A., Read, K., Edwards, P.M., 2022. Air pollution measurement errors: is your data fit for purpose? Atmos. Meas. Tech 15, 4091–4105. http://dx.doi.org/ 10.5194/amt-15-4091-2022.
- Duan, C., Liao, H., Wang, K., Ren, Y., 2023. The research hotspots and trends of volatile organic compound emissions from anthropogenic and natural sources: A systematic quantitative review. Environ. Res. 216, 114386. http://dx.doi.org/10. 1016/J.ENVRES.2022.114386.
- EC, 2010. Directive 2010/75/EU of the European parliament and of the council of 24 november 2010 on industrial emissions (integrated pollution prevention and control). URL: https://eur-lex.europa.eu/eli/dir/2010/75/oj/eng, (Last Accessed 03 March 2025).
- EC, 2024. Directive (EU) 2024/2881 of the European parliament and of the council of 23 october 2024 on ambient air quality and cleaner air for Europe. Off. J. Eur. Union URL: https://eur-lex.europa.eu/eli/dir/2024/2881/oj.
- EEA, 2023. Air quality e-reporting database. URL: https://www.eea.europa.eu/en/datahub/datahubitem-view/3b390c9c-f321-490a-b25a-ae93b2ed80c1, (Last Accessed 20 August 2024).

- Fagerli, H., Benedictow, A., Caspel, W.V., Gauss, M., Ge, Y., Jonson, J.E., Klein, H., Nyíri, Á., Simpson, D., Tsyro, S., Valdebenito, Á., Wind, P., Aas, W., Hjellbrekke, A., Solberg, S., Tørseth, K., Yttri, K.E., Matthews, B., Schindlbacher, S., Ullrich, B., Wankmüller, R., Klimont, Z., Scheuschner, T., Kuenen, J.J.P., Hellén, H., Jaffrezo, J.-L., Tusha, D., Mothes, F., Salameh, T., van Drooge, B.L., Wegener, R., 2023. EMEP Status Report 2023: Transboundary Particulate Matter, Photo-Oxidants, Acidifying and Eutrophying Components. Norwegian Meteorological Institute.
- Farhat, M., Afif, C., Zhang, S., Dusanter, S., Delbarre, H., Riffault, V., Sauvage, S., Borbon, A., 2024. Investigating the industrial origin of terpenoids in a coastal city in northern France: A source apportionment combining anthropogenic, biogenic, and oxygenated VOC. Sci. Total Environ. 928, 172098. http://dx.doi.org/10.1016/ J.SCITOTENV.2024.172098.
- Flemming, J., Huijnen, V., Arteta, J., Bechtold, P., Beljaars, A., Blechschmidt, A.-M., Diamantakis, M., Engelen, R.J., Gaudel, A., Inness, A., Jones, L., Josse, B., Katragkou, E., Marecal, V., Peuch, V.-H., Richter, A., Schultz, M.G., Stein, O., Tsikerdekis, A., 2015. Tropospheric chemistry in the integrated forecasting system of ECMWF. Geosci. Model. Dev. 8 (4), 975–1003.
- Foley, K.M., Roselle, S.J., Appel, K.W., Bhave, P.V., Pleim, J.E., Otte, T.L., Mathur, R., Sarwar, G., Young, J.O., Gilliam, R.C., Nolte, C.G., Kelly, J.T., Gilliland, A.B., Bash, J.O., 2010. Incremental testing of the community multiscale air quality (CMAQ) modeling system version 4.7. Geosci. Model. Dev. 3 (1), 205.
- Garatachea, R., Pay, M.T., Achebak, H., Jorba, O., Bowdalo, D., Guevara, M., Petetin, H., Ballester, J., García-Pando, C.P., 2024. National and transboundary contributions to surface ozone concentration across European countries. Commun. Earth Environ. 5:1, 1–17. http://dx.doi.org/10.1038/s43247-024-01716-w, URL: https://www.nature.com/articles/s43247-024-01716-w, 5.
- Ge, Y., Solberg, S., Heal, M.R., Reimann, S., Caspel, W.V., Hellack, B., Salameh, T., Simpson, D., 2024. Evaluation of modelled versus observed non-methane volatile organic compounds at European monitoring and evaluation programme sites in europe. Atmos. Chem. Phys. 24, 7699–7729. http://dx.doi.org/10.5194/ACP-24-7699-2024, URL: https://dacp.copernicus.org/articles/24/7699/2024/.
- Guenther, A.B., Jiang, X., Heald, C.L., Sakulyanontvittaya, T., Duhl, T., Emmons, L.K., Wang, X., 2012. The model of emissions of gases and aerosols from nature version 2.1 (MEGAN2.1): an extended and updated framework for modeling biogenic emissions. Geosci. Model. Dev. 1471–1492. http://dx.doi.org/10.5194/gmd-12-1885-2019.
- Guenther, A., Karl, T., Harley, P., Wiedinmyer, C., Palmer, P.I., Geron, C., 2006. Estimates of global terrestrial isoprene emissions using MEGAN (Model of Emissions of Gases and Aerosols from Nature. Atmos. Chem. Phys. 3138–3210. http://dx.doi.org/10.5194/acp-6-3181-2006.
- Guevara, M., Jorba, O., Tena, C., Gon, H.D.V.D., Kuenen, J., Elguindi, N., Darras, S., Granier, C., García-Pando, C.P., 2021. Copernicus atmosphere monitoring service temporal profiles (CAMS-TEMPO): Global and European emission temporal profile maps for atmospheric chemistry modelling. Earth Syst. Sci. Data 13, 367–404. http://dx.doi.org/10.5194/ESSD-13-367-2021.
- Guevara, M., Tena, C., Porquet, M., Jorba, O., García-Pando, C.P., 2019. HERMESv3, a stand-alone multi-scale atmospheric emission modelling framework-part 1: Global and regional module. Geosci. Model. Dev. 12, 1885–1907. http://dx.doi.org/10. 5194/GMD-12-1885-2019.
- Hanif, N.M., Hawari, N.S.S.L., Othman, M., Hamid, H.H.A., Ahamad, F., Uning, R., Ooi, M.C.G., Wahab, M.I.A., Sahani, M., Latif, M.T., 2021. Ambient volatile organic compounds in tropical environments: Potential sources, composition and impacts a review. Chemosphere 285, 131355. http://dx.doi.org/10.1016/J.CHEMOSPHERE. 2021.131355.
- Hartikainen, A., Yli-Pirilä, P., Tiitta, P., Leskinen, A., Kortelainen, M., Orasche, J., Schnelle-Kreis, J., Lehtinen, K.E., Zimmermann, R., Jokiniemi, J., Sippula, O., 2018. Volatile organic compounds from logwood combustion: Emissions and transformation under dark and photochemical aging conditions in a smog chamber. Environ. Sci. Technol. 52, 4979–4988. http://dx.doi.org/10.1021/ACS.EST.7B06269/ASSET/IMAGES/LARGE/ES-2017-06269B_0003.JPEG, URL: https://pubs.acs.org/doi/full/10.1021/acs.est.7b06269.
- Heald, C.L., Kroll, J.H., 2020. The fuel of atmospheric chemistry: Toward a complete description of reactive organic carbon. Sci. Adv. 6, http://dx.doi.org/10.1126/ SCIADV.AAY8967/SUPPL_FILE/AAY8967_SM.PDF, URL: https://www.science.org/ doi/10.1126/sciadv.aay8967.
- Heeley-Hill, A.C., Grange, S.K., Ward, M.W., Lewis, A.C., Owen, N., Jordan, C., Hodgson, G., Adamson, G., 2021. Frequency of use of household products containing VOCs and indoor atmospheric concentrations in homes. Env. Sci. Process. Impacts 23, 699–713. http://dx.doi.org/10.1039/D0EM00504E.
- Hersbach, H., Bell, B., Berrisford, P., Biavati, G., Horányi, A., Muñoz Sabater, J., Nicolas, J., Peubey, C., Radu, R., Rozum, I., Schepers, D., Simmons, A., Soci, C., Dee, D., Thépaut, J.-N., 2023. ERA5 hourly data on single levels from 1940 to present. http://dx.doi.org/10.24381/cds.adbb2d47, (Accessed on 3 January 2025).
- Huang, G., Brook, R., Crippa, M., Janssens-Maenhout, G., Schieberle, C., Dore, C., Guizzardi, D., Muntean, M., Schaaf, E., Friedrich, R., 2017. Speciation of anthropogenic emissions of non-methane volatile organic compounds: A global gridded data set for 1970–2012. Atmos. Chem. Phys. 17, 7683–7701. http://dx.doi.org/10.5194/ACP-17-7683-2017.

- Huang, R.J., Zhang, Y., Bozzetti, C., Ho, K.F., Cao, J.J., Han, Y., Daellenbach, K.R., Slowik, J.G., Platt, S.M., Canonaco, F., Zotter, P., Wolf, R., Pieber, S.M., Bruns, E.A., Crippa, M., Ciarelli, G., Piazzalunga, A., Schwikowski, M., Abbaszade, G., Schnelle-Kreis, J., Zimmermann, R., An, Z., Szidat, S., Baltensperger, U., Haddad, I.E., Prévôt, A.S., 2014. High secondary aerosol contribution to particulate pollution during haze events in China. Nat. 514, 218–222. http://dx.doi.org/10.1038/nature13774, VRI.: https://www.nature.com/articles/nature13774, 7521.
- Janjic, Z., Gall, R., 2012. Scientific documentation of the NCEP nonhydrostatic multiscale model on the B grid (NMMB). Part 1 Dynamics. University Corporation for Atmospheric Research, http://dx.doi.org/10.5065/D6WH2MZX, URL: https:// opensky.ucar.edu/islandora/object/technotes%3A502/.
- Juginović, A., Vuković, M., Aranza, I., Biloš, V., 2021. Health impacts of air pollution exposure from 1990 to 2019 in 43 European countries. Sci. Rep. 11, 1–15. http:// dx.doi.org/10.1038/s41598-021-01802-5, URL: https://www.nature.com/articles/ s41598-021-01802-5.
- Jung, D., de la Paz, D., Notario, A., Borge, R., 2022. Analysis of emissions-driven changes in the oxidation capacity of the atmosphere in Europe. Sci. Total Environ. 827, 154126. http://dx.doi.org/10.1016/J.SCITOTENV.2022.154126.
- Kelly, J.M., Doherty, R.M., O'Connor, F.M., Mann, G.W., 2018. The impact of biogenic, anthropogenic, and biomass burning volatile organic compound emissions on regional and seasonal variations in secondary organic aerosol. Atmos. Chem. Phys. 18, 7393–7422. http://dx.doi.org/10.5194/ACP-18-7393-2018.
- Klose, M., Jorba, O., Gonçalves Ageitos, M., Escribano, J., Dawson, M.L., Obiso, V., Di Tomaso, E., Basart, S., Montané Pinto, G., Macchia, F., Pérez García-Pando, C., 2021. MONARCH: Multiscale Online Nonhydrostatic Atmosphere Chemistry Model Version 2.0. Zenodo, http://dx.doi.org/10.5281/zenodo.5215467.
- Kuenen, J., Dellaert, S., Visschedijk, A., Jalkanen, J.P., Super, I., Gon, H.D.V.D., 2022.
 CAMS-REG-v4: a state-of-the-art high-resolution European emission inventory for air quality modelling. Earth Syst. Sci. Data 14, 491–515. http://dx.doi.org/10. 5194/FSSD-14-491-2022
- Lelieveld, J., Evans, J.S., Fnais, M., Giannadaki, D., Pozzer, A., 2015. The contribution of outdoor air pollution sources to premature mortality on a global scale. Nat. 525, 367–371. http://dx.doi.org/10.1038/nature15371, URL: https://www.nature.com/ articles/nature15371, 7569.
- Liaskoni, M., Huszár, P., Bartík, L., Perez, A.P.P., Karlický, J., Šindelářová, K., 2024. The long-term impact of biogenic volatile organic compound emissions on urban ozone patterns over central Europe: Contributions from urban and rural vegetation. Atmos. Chem. Phys. 24, 13541–13569. http://dx.doi.org/10.5194/ACP-24-13541-2024.
- Marques, B., Kostenidou, E., Valiente, A.M., Vansevenant, B., Sarica, T., Fine, L., Temime-Roussel, B., Tassel, P., Perret, P., Liu, Y., et al., 2022. Detailed speciation of non-methane volatile organic compounds in exhaust emissions from diesel and gasoline Euro 5 vehicles using online and offline measurements. Toxics 10 (4), 184.
- Miki, K., Itahashi, S., 2024. Enhanced O3 concentration due to biogenic emissions during a hot summer in 2018 over the Tokyo metropolitan area, Japan. Environ. Res. Commun. 6, 101015. http://dx.doi.org/10.1088/2515-7620/AD8399, URL: https://iopscience.iop.org/article/10.1088/2515-7620/ad8399, https://iopscience.iop.org/article/10.1088/2515-7620/ad8399/meta.
- Mills, G., Harmens, H., Wagg, S., Sharps, K., Hayes, F., Fowler, D., Sutton, M., Davies, B., 2016. Ozone impacts on vegetation in a nitrogen enriched and changing climate. Environ. Pollut. 208, 898–908. http://dx.doi.org/10.1016/J.ENVPOL.2015. 09.038.
- Ministry of Environment and Energy, 2024. Greece's Informative Inventory Report (IIR) 2024. Technical Report, Ministry of Environment and Energy, Athens, URL: https://cdr.eionet.europa.eu/gr/un/clrtap/iir/envzfrujq/2024_IIR_gr_.pdf/manage_document, (Accessed 14 December 2024).
- MITERD, 2020. Datos oficiales Calidad del Aire 2019. URL: https://www.miteco.gob.es/es/calidad-y-evaluacion-ambiental/temas/atmosfera-y-calidad-del-aire/calidad-del-aire/evaluacion-datos/datos/datos_oficiales_2019.html, (Last Accessed 20 August 2024).
- Monks, P.S., Archibald, A.T., Colette, A., Cooper, O., Coyle, M., Derwent, R., Fowler, D., Granier, C., Law, K.S., Mills, G.E., Stevenson, D.S., Tarasova, O., Thouret, V., Schneidemesser, E.V., Sommariva, R., Wild, O., Williams, M.L., 2015. Tropospheric ozone and its precursors from the urban to the global scale from air quality to short-lived climate forcer. Atmos. Chem. Phys. 15, 8889–8973. http://dx.doi.org/10.5194/ACP-15-8889-2015.
- Navarro-Barboza, H., Pandolfi, M., Guevara, M., Enciso, S., Tena, C., Via, M., Yus-Díez, J., Reche, C., Pérez, N., Alastuey, A., Querol, X., Jorba, O., 2024. Uncertainties in source allocation of carbonaceous aerosols in a Mediterranean region. Environ. Int. 183, 108252. http://dx.doi.org/10.1016/j.envint.2023.108252.
- NEPA, 2024. Romania's Informative Inventory Report 1990–2022. Technical Report, National Environmental Protection Agency of Romania, URL: https://webdab01.umweltbundesamt.at/download/submissions2024/RO_IIR2024. zip?cgiproxy_skip=1, (Accessed 14 December 2024).
- Oliveira, K., Guevara, M., Jorba, O., Petetin, H., Bowdalo, D., Tena, C., Pinto, G.M., López, F., García-Pando, C.P., 2024. On the uncertainty of anthropogenic aromatic volatile organic compound emissions: Model evaluation and sensitivity analysis. Atmos. Chem. Phys. 24, 7137–7177. http://dx.doi.org/10.5194/ACP-24-7137-2024.
- Oliveira, K., Guevara, M., Jorba, O., Querol, X., García-Pando, C.P., 2023. A new NMVOC speciated inventory for a reactivity-based approach to support ozone control strategies in Spain. Sci. Total Environ. 867, 161449. http://dx.doi.org/10.1016/

- j.scitotenv.2023.161449, URL: https://www.sciencedirect.com/science/article/pii/ S0048969723000645
- Oliveira, K., Guevara, M., Kuenen, J., Jorba, O., Pérez García-Pando, C., Denier van der Gon, H., 2025. Oliveiraetal NMVOC split for CAMS-REGv7.1. Zenodo, http://dx.doi.org/10.5281/zenodo.15019284.
- Olivier, J.G.J., A. F., B., der Maas, C.W.M.V., Berdowski, J.J.M., Veldt, C., Bloos, J.P.J., Visschedijk, A.J.H., P. Y. J., Z., Haverlag, J.L., 1996. Description of EDGAR version 2.0. URL: https://www.rivm.nl/bibliotheek/rapporten/771060002.pdf.
- Panopoulou, A., Liakakou, E., Sauvage, S., Gros, V., Locoge, N., Stavroulas, I., Bonsang, B., Gerasopoulos, E., Mihalopoulos, N., 2020. Yearlong measurements of monoterpenes and isoprene in a mediterranean city (athens): Natural vs anthropogenic origin. Atmos. Environ. 243, 117803. http://dx.doi.org/10.1016/J. ATMOSENV.2020.117803.
- Passant, N., 2002. Speciation of UK Emissions of Non-Methane Volatile Organic Compounds. AEA Technology.
- Peng, Y., Mouat, A.P., Hu, Y., Li, M., McDonald, B.C., Kaiser, J., 2022. Source appointment of volatile organic compounds and evaluation of anthropogenic monoterpene emission estimates in Atlanta, Georgia. Atmos. Environ. 288, http://dx.doi.org/10.1016/J.ATMOSENV.2022.119324, URL: https://repository.library.noaa.gov/view/noaa/49805.
- Pérez, C., Haustein, K., Janjic, Z., Jorba, O., Huneeus, N., Baldasano, J.M., Black, T., Basart, S., Nickovic, S., Miller, R.L., Perlwitz, J.P., Schulz, M., Thomson, M., 2011. Atmospheric dust modeling from meso to global scales with the online NMMB/BSC-Dust model; part 1: Model description, annual simulations and evaluation. Atmos. Chem. Phys. 11 (24), 13001–13027. http://dx.doi.org/10.5194/acp-11-13001-2011, URL: https://acp.copernicus.org/articles/11/13001/2011/.
- Pernigotti, D., Georgieva, E., Thunis, P., Bessagnet, B., 2012. Impact of meteorology on air quality modeling over the Po valley in northern Italy. Atmos. Environ. 51, 303–310. http://dx.doi.org/10.1016/j.atmosenv.2011.12.059, URL: https://www. sciencedirect.com/science/article/pii/S1352231011013495.
- Petetin, H., Guevara, M., Garatachea, R., López, F., Oliveira, K., Enciso, S., Jorba, O., Querol, X., Massagué, J., Alastuey, A., García-Pando, C.P., 2023. Assessing ozone abatement scenarios in the framework of the Spanish ozone mitigation plan. Sci. Total Environ. 902, 165380. http://dx.doi.org/10.1016/J.SCITOTENV.2023. 165380.
- Pozzer, A., Reifenberg, S.F., Kumar, V., Franco, B., Kohl, M., Taraborrelli, D., Gromov, S., Ehrhart, S., Jöckel, P., Sander, R., Fall, V., Rosanka, S., Karydis, V., Akritidis, D., Emmerichs, T., Crippa, M., Guizzardi, D., Kaiser, J.W., Clarisse, L., Kiendler-Scharr, A., Tost, H., Tsimpidi, A., 2022. Simulation of organics in the atmosphere: evaluation of EMACv2.54 with the Mainz Organic Mechanism (MOM) coupled to the ORACLE (v1.0) submodel. Geosci. Model. Dev. 15, 2673–2710. http://dx.doi.org/10.5194/GMD-15-2673-2022.
- RIVM, 2024. Air monitoring network dataset. URL: https://data.rivm.nl/data/luchtmeetnet/, (Last Accessed 20 August 2024).
- Rowlinson, M.J., Evans, M.J., Carpenter, L.J., Read, K.A., Punjabi, S., Adedeji, A., Fakes, L., Lewis, A., Richmond, B., Passant, N., Murrells, T., Henderson, B., Bates, K.H., Helmig, D., 2024. Revising VOC emissions speciation improves the simulation of global background ethane and propane. Atmos. Chem. Phys. 24, 8317–8342. http://dx.doi.org/10.5194/ACP-24-8317-2024, URL: https://acp.copernicus.org/articles/24/8317/2024/.
- Sarwar, G., Simon, H., Bhave, P., Yarwood, G., 2012. Examining the impact of heterogeneous nitryl chloride production on air quality across the United States. Atmos. Chem. Phys. 12 (14), 6455–6473.
- von Schneidemesser, E., McDonald, B.C., van der Gon, H.D., Crippa, M., Guizzardi, D., Borbon, A., Dominutti, P., Huang, G., Jansens-Maenhout, G., Li, M., Ou-Yang, C.F., Tisinai, S., Wang, J.L., 2023. Comparing urban anthropogenic NMVOC measurements with representation in emission inventories—A global perspective. J. Geophys. Res. Atmos. 128, e2022JD037906. http://dx.doi.org/10.1029/2022JD037906, URL: https://onlinelibrary.wiley.com/doi/fubs/10.1029/2022JD037906, https://onlinelibrary.wiley.com/doi/abs/10.1029/2022JD037906, https://agupubs.onlinelibrary.wiley.com/doi/10.1029/2022JD037906.
- Schultz, M., 2007. Reanalysis of the tropospheric chemical composition over the past 40 years. In: Schultz, M.G. (Ed.), Max Planck Institute for Meteorology, Jülich/Hamburg.
- Shuai, J., Kim, S., Ryu, H., Park, J., Lee, C.K., Kim, G.B., Ultra, V.U., Yang, W., 2018. Health risk assessment of volatile organic compounds exposure near Daegu dyeing industrial complex in South Korea. BMC Public Health 18, 1–13. http://dx.doi.org/10.1186/S12889-018-5454-1/TABLES/7, URL: https://bmcpublichealth.biomedcentral.com/articles/10.1186/s12889-018-5454-1.
- Sindelarova, K., Markova, J., Simpson, D., Huszar, P., Karlicky, J., Darras, S., Granier, C., 2022. High-resolution biogenic global emission inventory for the time period 2000–2019 for air quality modelling. Earth Syst. Sci. Data 14, 251–270. http://dx.doi.org/10.5194/ESSD-14-251-2022.

- Skoulidou, I., Segers, A., Henzing, B., Zhang, J., Goudriaan, R., Koukouli, M.E., Balis, D., 2024. Towards integration of LOTOS-EUROS high resolution simulations and heterogenous low-cost sensor observations. Atmos. Environ. 333, 120652. http://dx.doi.org/10.1016/J.ATMOSENV.2024.120652.
- Srivastava, D., Vu, T.V., Tong, S., Shi, Z., Harrison, R.M., 2022. Formation of secondary organic aerosols from anthropogenic precursors in laboratory studies. Npj Clim. Atmos. Sci. 5, 1–30. http://dx.doi.org/10.1038/s41612-022-00238-6, URL: https://www.nature.com/articles/s41612-022-00238-6.
- Stackelberg, K.V., Buonocore, J., Bhave, P.V., Schwartz, J.A., 2013. Public health impacts of secondary particulate formation from aromatic hydrocarbons in gasoline. Environ. Heal. 12, 19. http://dx.doi.org/10.1186/1476-069X-12-19, URL: , https://www.ncbi.nlm.nih.gov/pmc/articles/PMC3652775/.
- Stockwell, C.E., Veres, P.R., Williams, J., Yokelson, R.J., 2015. Characterization of biomass burning emissions from cooking fires, peat, crop residue, and other fuels with high-resolution proton-transfer-reaction time-of-flight mass spectrometry. Atmos. Chem. Phys. 15 (2), 845–865. http://dx.doi.org/10.5194/acp-15-845-2015.
- Tai, A.P., Sadiq, M., Pang, J.Y., Yung, D.H., Feng, Z., 2021. Impacts of surface ozone pollution on global crop yields: Comparing different ozone exposure metrics and incorporating co-effects of CO2. Front. Sustain. Food Syst. 5, 534616. http://dx.doi.org/10.3389/FSUFS.2021.534616/BIBTEX, URL: www.frontiersin.org.
- Thangavel, P., Park, D., Lee, Y.C., 2022. Recent insights into particulate matter (PM2.5)-mediated toxicity in humans: An overview. Int. J. Environ. Res. Public Heal. 19, http://dx.doi.org/10.3390/IJERPH19127511, URL: https://www.ncbi.nlm.nih.gov/pmc/articles/PMC9223652/.
- Theloke, J., Friedrich, R., 2007. Compilation of a database on the composition of anthropogenic VOC emissions for atmospheric modeling in Europe. Atmos. Environ. 41 (19), 4148–4160.
- Thunis, P., Crippa, M., Cuvelier, C., Guizzardi, D., de Meij, A., Oreggioni, G., Pisoni, E., 2021. Sensitivity of air quality modelling to different emission inventories: A case study over Europe. Atmos. Environ. X 10, 100111. http://dx.doi.org/10.1016/J. AEAOA.2021.100111.
- Timmermans, R., van Pinxteren, D., Kranenburg, R., Hendriks, C., Fomba, K.W., Herrmann, H., Schaap, M., 2022. Evaluation of modelled LOTOS-EUROS with observational based PM10 source attribution. Atmos. Environ. X 14, 100173. http://dx.doi.org/10.1016/J.AEAOA.2022.100173.
- Tokaya, J., Kranenburg, R., Timmermans, R., Coenen, P., Kelly, B., Hullegie, J., Megaritis, T., Valastro, G., 2024. The impact of shipping on the air quality in European port cities with a detailed analysis for Rotterdam. Atmos. Environ. X 23, 100278. http://dx.doi.org/10.1016/J.AEAOA.2024.100278.
- Trimmel, H., Hamer, P., Mayer, M., Schreier, S.F., Weihs, P., Eitzinger, J., Sandén, H., Fitzky, A.C., Richter, A., Calvet, J.C., Bonan, B., Meurey, C., Vallejo, I., Eckhardt, S., Santos, G.S., Oumami, S., Arteta, J., Marécal, V., Tarrasón, L., Karl, T., Rieder, H.E., 2023. The influence of vegetation drought stress on formaldehyde and ozone distributions over a central European city. Atmos. Environ. 304, 119768. http://dx.doi.org/10.1016/J.ATMOSENV.2023.119768.
- Wesely, M., 1989. Parameterization of surface resistances to gaseous dry deposition in regional-scale numerical models. Atmos. Environ. (1967) 23 (6), 1293–1304.
- Wild, O., Zhu, X., Prather, M.J., 2000. Fast-J: Accurate simulation of in-and below-cloud photolysis in tropospheric chemical models. J. Atmos. Chem. 37 (3), 245–282.
- Xiao, Z., Yang, X., Gu, H., Hu, J., Zhang, T., Chen, J., Pan, X., Xiu, G., Zhang, W., Lin, M., 2024. Characterization and sources of volatile organic compounds (VOCs) during 2022 summer ozone pollution control in Shanghai, China. Atmos. Environ. 327, http://dx.doi.org/10.1016/J.ATMOSENV.2024.120464, URL: https://typeset. io/papers/characterization-and-sources-of-volatile-organic-compounds-52qlj62i2b.
- Xiong, Y., Du, K., Huang, Y., 2024. One-third of global population at cancer risk due to elevated volatile organic compounds levels. Npj Clim. Atmos. Sci. 7, 1–11. http://dx.doi.org/10.1038/s41612-024-00598-1, URL: https://www.nature. com/articles/s41612-024-00598-1.
- Yarwood, G., Rao, S., Yocke, M., Whitten, G.Z., 2005. Updates to the Carbon Bond Chemical Mechanism: CB05. Final Report to the US EPA, 1130RT-0400675, 8, p. 13.
- Ye, F., Li, J., Gao, Y., Wang, H., An, J., Huang, C., Guo, S., Lu, K., Gong, K., Zhang, H., Qin, M., Hu, J., 2024. The role of naphthalene and its derivatives in the formation of secondary organic aerosol in the Yangtze River Delta region, China. Atmos. Chem. Phys. 24, 7467–7479. http://dx.doi.org/10.5194/ACP-24-7467-2024.
- Zhang, X., Stocker, J., Johnson, K., Fung, Y.H., Yao, T., Hood, C., Carruthers, D., Fung, J.C., 2022. Implications of mitigating ozone and fine particulate matter pollution in the Guangdong-Hong Kong-Macau Greater Bay Area of China using a regional-to-local coupling model. GeoHealth 6, http://dx.doi.org/10.1029/2021GH000506.
- Zhou, X., Zhou, X., Wang, C., Zhou, H., 2023. Environmental and human health impacts of volatile organic compounds: A perspective review. Chemosphere 313, 137489. http://dx.doi.org/10.1016/J.CHEMOSPHERE.2022.137489.